Midkine in chick and mouse retinas: neuroprotection, glial reactivity and the formation of Müller glia-derived progenitor cells

Warren A. Campbell[1], Amanda Fritsch-Kelleher[1], Isabella Palazzo[1], Thanh Hoang[2], Seth Blackshaw[2], Andy J. Fischer[1]*

1 Department of Neuroscience, College of Medicine, The Ohio State University, Columbus, OH

2 Solomon H. Snyder Department of Neuroscience, Johns Hopkins University School of Medicine, Baltimore, MD

***corresponding author**: Andy J. Fischer, Department of Neuroscience, Ohio State University, College of Medicine, 3020 Graves Hall, 333 W. 10th Ave, Columbus, OH 43210-1239, USA. Telephone: (614) 292-3524; Fax: (614) 688-8742; email: Andrew.Fischer@osumc.edu

Abbreviated title: Midkine in Müller glia and Müller glia-derived progenitor cells

Number of pages: 69 **Number of Figures**: 12 **Number of Supplemental Figures**: 6 **Number of Tables:** 2

Author Contributions: WAC, AF-K and IP designed and executed experiments, gathered data, constructed figures and contributed to writing the manuscript. TH and SB executed experiments, and gathered data. AJF designed experiments, analyzed data, constructed figures and wrote the manuscript.

Acknowledgements: This work was supported by RO1 EY022030-08 (AJF) and UO1 EY027267-04 (SB, AJF).

Abstract

Recent studies have shown that midkine (MDK), a basic heparin-binding growth factor, is involved in the development and regeneration of the zebrafish retina. However, very little is known about MDK in the retinas of warm-blooded vertebrates. We investigate the expression patterns of MDK and related factors, roles in neuronal survival, and influence upon the formation of Müller glia-derived progenitor cells (MGPCs) in chick and mouse model systems. By using single-cell RNA-sequencing, we find that *MDK* is upregulated during Müller glia (MG) maturation in chick development and when stimulated to reprogram into MGPCs after NMDA damage or FGF2/Insulin treatment. Interestingly, *MDK* is significantly up-regulated by MG in damaged chick retinas, but down-regulated by MG in damaged mouse retinas. In both chick and mouse retinas, exogenous MDK selectively up-regulates cFOS and pS6 (a readout of mTOR-signaling) in MG. In the chick, intraocular injections of MDK before injury is neuroprotective with an observed decrease in dying neurons and microglial reactivity, inducing fewer proliferating MGPCs. Blocking MDK signaling with Na_3VO_4 following blocks neuroprotective effects with an increase the number of dying cells and negates the pro-proliferative effects on MGPCs. Inhibitors of PP2A and Pak1 associated with MDK integrin β1 signaling had MG specific inhibitory effects on MGPC formation. In mice, MDK administration with NMDA damage drives a small but significant increase in MGPCs. We conclude that *MDK* expression is dynamically regulated in reactive Müller glia and during reprogramming into MGPCs. MDK acts to coordinate glial activity, neuronal survival, and may act in an autocrine manner to influence the re-programming of Müller glia into proliferating MGPCs.

Introduction

Midkine (MDK) and pleiotrophin (PTN) are secreted factors that belong to a family of basic heparin-binding cytokines (Muramatsu, 2002). The C-terminal domain of MDK interacts with carbohydrate-bindings proteins which facilitate dimerization and cell signaling (Fabri et al., 1993; Iwasaki et al., 1997; Kilpeläinen et al., 2000; Tsutsui et al., 1991). Extracellular matrix proteoglycans that have a high binding-affinity for MDK include protein tyrosine phosphatase-ζ receptor-like 1 (PTPRZ1), syndecans, glypican-2, PG-M/versican, integrin $\alpha_6\beta_1$, low density lipoprotein receptor-related protein (LRP), and neuroglycans (Ichihara-Tanaka et al., 2006; Kojima et al., 1996; Kurosawa et al., 2001; Maeda et al., 1999; Mitsiadis et al., 1995; Muramatsu et al., 2000; Muramatsu et al., 2004; Nakanishi et al., 1997; Zou et al., 2000). MDK forms a complex with these proteoglycans to initiate cell-signaling through receptor tyrosine kinases and activation of second messengers such as src, PI-3K, and PAK1 (Qi et al., 2001; Shen et al., 2015; Thillai et al., 2016).

During development the roles of MDK are conserved across many vertebrate species including fish, mice, and humans (Tsutsui et al., 1991). MDK has different functions including promoting cell survival and the proliferation of stem cells, acting directly on stem cells during normal fetal development and organogenesis (Mitsiadis et al., 1995). MDK has been implicated in the pathogenesis of more than 20 different types of cancers, resistance to chemotherapeutics, increased survival of cancerous cells with acidosis and hypoxia, and elevated levels of MDK have been correlated with poor prognoses (Dai et al., 2009; Kang et al., 2004; Mashima et al., 2009; Mirkin et al., 2005; Reynolds et al., 2004; Salama et al., 2006; Takei et al., 2001; Takei et al., 2006; Tsutsui et al., 1993). In damaged mammalian CNS, MDK expression is elevated and may support neuronal survival (Jochheim-Richter et al., 2006; Kikuchi-Horie et al., 2004; Miyashiro et al., 1998; Obama et al., 1998; Sakakima et al., 2006). In rodent eyes, subretinal delivery of MDK protects photoreceptors from light-mediated degeneration (Unoki et al., 1994). In sum, MDK has pleotropic functions that are context-dependent.

In fish, retinal regeneration is a robust process that restores neurons and visual function following damage, whereas this process is far less robust in birds and nearly absent in mammals (Hitchcock and Raymond, 1992; Karl et al., 2008; Raymond, 1991).

Müller glia (MG) have been identified as the cell-of-origin for progenitors in mature retinas (Bernardos et al., 2007; Fausett and Goldman, 2006; Fausett et al., 2008; Fischer and Reh, 2001; Ooto et al., 2004). In mammalian retina, significant stimulation, such as forced expression of Ascl1, inhibition of histone deacetylases and neuronal damage, is required to reprogram MG into progenitor-like cells (Karl et al., 2008; Pollak et al., 2013, 1; Ueki et al., 2015). In the chick retina, MG readily reprogram into progenitor-like cells that proliferate, but the progeny have a limited capacity to differentiate as neurons (Fischer and Reh, 2001; Fischer and Reh, 2003). Understanding the mechanisms that regulate the proliferation and differentiation of MGPCs is important to harnessing the regenerative potential of MG in warm-blooded vertebrates.

Recent studies in zebrafish retina have indicated that MDK-a and MDK-b are up-regulated in stem niches and in MG during reprogramming (Calinescu et al., 2009). MDK-a is expressed by mitotic retinal progenitors at 30 hrs post-fertilization, then in MG at 72 hrs post-fertilization through adulthood (Gramage et al., 2014). Knock-down of MDK-b results in microphthalmia or anophthalmia (Calinescu et al., 2009). During reprogramming of MG into MGPCs following retinal damage, MDK-a controls cell cycle exit and neuronal differentiation via bHLH transcription factor Id2a (Luo et al., 2012; Nagashima et al., 2019). Nothing is known about how MDK influences the process of retinal regeneration in warm-blooded vertebrates. Accordingly, we investigate expression patterns and the impact of MDK on glial cells in the chick and mouse retinas *in vivo*.

Methods and Materials:

Animals:

The animals approved for use in these experiments was in accordance with the guidelines established by the National Institutes of Health and IACUC at The Ohio State University. Newly hatched P0 wildtype leghorn chicks (*Gallus gallus domesticus*) were obtained from Meyer Hatchery (Polk, Ohio). Post-hatch chicks were maintained in a regular diurnal cycle of 12 hours light, 12 hours dark (8:00 AM-8:00 PM). Chicks were housed in stainless-steel brooders at 25°C and received water and Purina^{tm} chick

starter *ad libitum*. Mice were kept on a cycle of 12 h light, 12 h dark (lights on at 6:00 AM). C57BL/6J mice between the ages of P60-P100 were used for all experiments.

Fertilized eggs were obtained from the Michigan State University, Department of Animal Science. Eggs were incubated at a constant 37.5°C, with a 1hr period room temperature cool down every 24hrs. Additionally, the eggs were rocked every 45 minutes, and held at a constant relative humidity of 45%. Embryos were harvested at various time points after incubation and staged according to guidelines established by Hamburger and Hamilton (1951).

Intraocular injections:

Chicks were anesthetized with 2.5% isoflurane mixed with oxygen from a non-rebreathing vaporizer. The technical procedures for intraocular injections were performed as previously described (Fischer et al., 1998). With all injection paradigms, both pharmacological and vehicle treatments were administered to the right and left eye respectively. Compounds were injected in 20 μl sterile saline with 0.05 mg/ml bovine serum albumin added as a carrier. For mice injections, the total volume injected into each eye was 2μl. The details of compounds injected in to the vitreous are described (Table S1)

Preparation of clodronate liposomes:

Clodronate liposomes were synthesized utilizing a modified protocol from previous descriptions (Van Rooijen, 1989; van Rooijen, 1992; Zelinka et al., 2012). In short, approximately 8 mg of L-α-Phosphatidyl-DL-glycerol sodium salt (Sigma P8318) was dissolved in chloroform. 50 mg of cholesterol was dissolved in chloroform with the lipids in a sterile microcentrifuge tube. This tube was rotated under nitrogen gas to evaporate the chloroform and leave a thin lipid-film on the walls of the tube. 158 mg dichloro-methylene diphosphonate (clodronate; Sigma-Aldrich) dissolved sterile PBS (pH 7.4) was added to the lipid/cholesterol film and vortexed for 5 minutes. To reduce size variability of lipid vesicles, the mixture was sonicated at 42 kHz for 6 minutes. Purification of liposomes was accomplished via centrifugation at 10,000 x G for 15 minutes, aspirated, and resuspended in 150 μl PBS. Each retinal injection used

between 5 and 20 ul of clodronate-liposome solution. There was a variable yield of clodronate-liposomes during the purification resulting in some variability per dose. The dosage was adjusted such that >98% of the microglia are ablated by 2 days after administration with no off-target cell death or pigmented epithelial cells.

Single Cell RNA sequencing of retinas

Retinas were obtained from embryonic, postnatal chick, and adult mouse retinas. Isolated retinas were dissociated in a 0.25% papain solution in Hank's balanced salt solution (HBSS), pH = 7.4, for 30 minutes, and suspensions were frequently triturated. The dissociated cells were passed through a sterile 70µm filter to remove large particulate debris. Dissociated cells were assessed for viability (Countess II; Invitrogen) and cell-density diluted to 700 cell/µl. Each single cell cDNA library was prepared for a target of 10,000 cells per sample. The cell suspension and Chromium Single Cell 3' V2 reagents (10X Genomics) were loaded onto chips to capture individual cells with individual gel beads in emulsion (GEMs) using 10X Chromium Controller. cDNA and library amplification for an optimal signal was 12 and 10 cycles respectively. Sequencing was conducted on Illumina HiSeq2500 (Genomics Resource Core Facility, John's Hopkins University) or HiSeq4000 (Novogene) with 26 bp for Read 1 and 98 bp for Read 2. Fasta sequence files were de-multiplexed, aligned, and annotated using the chick ENSMBL database (GRCg6a, Ensembl release 94) or mouse ENSMBL database (GRCm38.p6, Ensembl release 67) and Cell Ranger software. Gene expression was counted using unique molecular identifier bar codes, and gene-cell matrices were constructed. Using Seurat toolkits, t-distributed stochastic neighbor embedding (tSNE) plots or Uniform Manifold Approximation and Projection for Dimension Reduction (UMAP) plots were generated from aggregates of multiple scRNA-seq libraries (Butler et al., 2018; Satija et al., 2015). Compiled in each tSNE/UMAP plot are two biological library replicates for each experimental condition. Seurat was used to construct violin/scatter plots. Significance of difference in violin/scatter plots was determined using a Wilcoxon Rank Sum test with Bonferroni correction. Monocle was used to construct unbiased pseudo-time trajectories and scatter plotters for MG and MGPCs across pseudotime (Qiu et al., 2017a; Qiu et al., 2017b; Trapnell et al., 2012). Genes that were

used to identify different types of retinal cells included the following: (1) Müller glia: *GLUL, VIM, SCL1A3, RLBP1*, (2) MGPCs: *PCNA, CDK1, TOP2A, ASCL1*, (3) microglia: *C1QA, C1QB, CCL4, CSF1R, TMEM22*, (4) ganglion cells: *THY1, POU4F2, RBPMS2, NEFL, NEFM*, (5) amacrine cells: *GAD67, CALB2, TFAP2A*, (6) horizontal cells: *PROX1, CALB2, NTRK1*, (7) bipolar cells: *VSX1, OTX2, GRIK1, GABRA1*, and (7) cone photoreceptors: *CALB1, GNAT2, OPN1LW*, and (8) rod photoreceptors: *RHO, NR2E3, ARR3.* The MG have an over-abundant representation in the scRNA-seq databases. This likely resulted from fortuitous capture-bias and/or tolerance of the MG to the dissociation process. Single cell libraries for NMDA and FGF insulin in the mouse and chick generated by our lab have first been reported for cross species comparisons (Hoang et al., 2019), where chick embryonic retinal libraries are first being reported in this study.

Fixation, sectioning and immunocytochemistry:

Retinal tissue samples were formaldehyde fixed, sectioned, and labeled via immunohistochemistry as described previously (Fischer et al., 2008; Fischer et al., 2009a). Antibody dilutions and commercial sources for images used in this study are described (Table S2). Observed labeling was not due to off-target labeling of secondary antibodies or tissue autofluorescence because sections incubated exclusively with secondary antibodies were devoid of fluorescence. Secondary antibodies utilized include donkey-anti-goat-Alexa488/568, goat-anti-rabbit-Alexa488/568/647, goat-anti-mouse-Alexa488/568/647, goat-anti-rat-Alexa488 (Life Technologies) diluted to 1:1000 in PBS and 0.2% Triton X-100.

Labeling for EdU:

For the detection of nuclei that incorporated EdU, immunolabeled sections were fixed in 4% formaldehyde in 0.1M PBS pH 7.4 for 5 minutes at room temperature. Samples were washed for 5 minutes with PBS, permeabilized with 0.5% Triton X-100 in PBS for 1 minute at room temperature and washed twice for 5 minutes in PBS. Sections were incubated for 30 minutes at room temperature in a buffer consisting of 100 mM

Tris, 8 mM $CuSO_4$, and 100 mM ascorbic acid in dH_2O. The Alexa Fluor 568 Azide (Thermo Fisher Scientific) was added to the buffer at a 1:100 dilution.

Terminal deoxynucleotidyl transferase dUTP nick end labeling (TUNEL):

The TUNEL assay was implemented to identify dying cells by imaging fluorescent labeling of double stranded DNA breaks in nuclei. The *In Situ* Cell Death Kit (TMR red; Roche Applied Science) was applied to fixed retinal sections as per the manufacturer's instructions.

Photography, measurements, cell counts and statistics:

Microscopy images of retinal sections were captured with the Leica DM5000B microscope with epifluorescence and the Leica DC500 digital camera. High resolution confocal images were obtained with a Leica SP8 available in The Department of Neuroscience Imaging Facility at The Ohio State University. Representative images are modified to have enhanced color, brightness, and contrast for improved clarity using Adobe Photoshop. In EdU proliferation assays, a fixed region of retina was counted and average numbers of Sox2 and EdU co-labeled cells. The retinal region selected for investigation was standardized between treatment and control groups to reduce variability and improve reproducibility.

Similar to previous reports (Fischer et al., 2009a; Fischer et al., 2009b; Ghai et al., 2009), immunofluorescence was quantified by using ImagePro6.2 (Media Cybernetics, Bethesda, MD, USA) or Image J (NIH). Identical illumination, microscope, and camera settings were used to obtain images for quantification. Retinal areas were sampled from 5.4 MP digital images. These areas were randomly sampled over the inner nuclear layer (INL) where the nuclei of the bipolar and amacrine neurons were observed. Measurements of immunofluorescence were performed using ImagePro 6.2 as described previously (Ghai et al., 2009; Stanke et al., 2010; Todd and Fischer, 2015). The density sum was calculated as the total of pixel values for all pixels within thresholded regions. The mean density sum was calculated for the pixels within threshold regions from ≥5 retinas for each experimental condition. GraphPad Prism 6 was used for statistical analyses.

Measurement for immunofluorescence of cFos in the nuclei of MG/MGPCs were made by from single optical confocal sections by selecting the total area of pixel values above threshold (≥70) for Sox2 or Sox9 immunofluorescence (in the red channel) and copying nuclear cFos from only MG (in the green channel). The MG-specific cFos was quantified (as described below or copied onto a 70% grayscale background for figures. Measurements of pS6 immunofluorescence were made for a fixed, cropped area (14,000 μm^2) of INL, OPL and ONL. Measurements were made for regions containing pixels with intensity values of 70 or greater (0 = black and 255 = saturated). The total area was calculated for regions with pixel intensities above threshold. The intensity sum was calculated as the total of pixel values for all pixels within threshold regions. The mean intensity sum was calculated for the pixels within threshold regions from ≥5 retinas for each experimental condition.

For statistical evaluation of differences in treatments, a two-tailed paired *t*-test was applied for intra-individual variability where each biological sample also served as its own control. For two treatment groups comparing inter-individual variability, a two-tailed unpaired *t*-test was applied. For multivariate analysis, an ANOVA with the associated Tukey Test was used to evaluate any significant differences between multiple groups.

Results:

***MDK* and *PTN* in embryonic retina:**

scRNA-seq retina libraries were established at four stages of development including E5, E8, E12, and E15. The aggregation of these libraries yielded 22,698 cells after filtering to exclude doublets, cells with low UMI, and low genes/cell. UMAP plots of aggregate libraries of embryonic retinas formed clustered of cells into patterns that correlated to both developmental stage and cell type (Fig. 1a). Cell types were identified based on expression of well-established markers. Specifically, retinal progenitor cells from E5 and E8 retinas were identified by expression of *ASCL1*, C*DK1*, and *TOP2A*. (Supplemental Fig. 1a,b). Maturing MG were identified by expression of *GLUL*, *RLBP1* and *SLC1A3* (Supplemental Fig. 1a,b).

Elevated levels of *MDK* expression were observed in MG at E12 and E15, with lower levels of expression in immature MG at E8 and retinal progenitor cells at E5 (Fig. 1c,d). *PTN* was prominently expressed in immature and mature MG, but was also detected in immature amacrine cells (E8), rod photoreceptors (E12), and cone photoreceptors (E15) (Fig. 1c). Levels of *MDK* and *PTN* were significantly higher in maturing MG compared to immature MG and RPCs (Fig. 1d). Putative receptors and signal transducers of MDK and PTN include integrin β1 (*ITGB1*), receptor-like protein tyrosine phosphatase-ζ (*PTPRZ1*), chondroitin sulfate proteoglycan 5 (*CSPG5*) and p21-activated serine/threonine kinase (*PAK1*). These mRNAs had variable, scattered expression in embryonic retinal cells. Scattered expression of *PTPRZ1*, *ITGB1* and *PAK1* was observed in RPCs, immature and mature MG (Supplemental Fig. 1c). *CSPG5* was expressed by developing photoreceptors, amacrine, ganglion and bipolar cells (Fig. 1c). Additionally, *CSPG5* was expressed at significantly elevated levels by immature and maturing MG compared to levels in RPCs (Fig. 1c.d).

Re-embedding of RPCs and MG for pseudotime analysis revealed a trajectory of cells with early RPCs and maturing MG at opposite ends of the trajectory (Fig. 1e). Across the pseudotime trajectory levels of *GLUL* increased, while levels of *CDK1* decreased (Supplemental Fig. 1e,f). Similar to the pattern of expression of *GLUL*, the expression of *MDK* and *PTN* increases from retinal progenitors to maturing MG (Fig. 1e,f). Higher levels of expression were observed for both *MDK* and *PTN*, with *PTN* at low levels in retinal progenitors (Fig. 1f,g). Across pseudotime, levels of *MDK* were high in early progenitors, with a dip in expression during transition phases, and increased in maturing MG (Fig. 1f,g). Collectively, these findings suggest that both *PTN* and *MDK* are up-regulated by maturing MG during late stages of embryonic development, and, based on patterns of expression of putative receptors, MDK and PTN may have autocrine and paracrine actions in late-stage embryonic chick retina.

Upregulation MDK in MG of damaged retinas

scRNA-seq libraries were aggregated for retinal cells obtained from control and NMDA-damaged retinas at various time points (24, 48 and 72 hrs) after treatment (Fig. 2a). UMAP plots were generated and clusters of different cells were identified based on

well-established patterns of expression (Fig. 2a,b). For example, resting MG formed a discrete cluster of cells and expressed high levels of *GLUL, RLBP1* and *SLC1A3* (Supplemental Fig. 2a,b). After damage, MG down-regulate markers of mature glia as they transition into reactive glial cells and into progenitor-like cells that up-regulate *TOP2A, CDK1* and *ESPL1* (Supplemental Fig. 2a,b). *MDK* was expressed at low levels in relatively few resting MG in undamaged retina, unlike maturing MG in late stages of embryonic retinas (Fig. 1c,e), suggesting a down-regulation of *MDK* in MG as development proceeds after hatching. The expression of *MDK* was scattered in oligodendrocytes and Non-astrocytic Inner Retinal Glia (NIRGs). NIRG cells are a distinct type of glial cells that has been described in the retinas of birds (Rompani and Cepko 2010; Fischer et al., 2010) and some types of reptiles (Todd et al., 2016). Following NMDA-induced damage, *MDK* is upregulated in MG and MGPCs at 24hrs, 48hrs, and 72hrs after treatment (Fig. 2c,e). In addition, MGPCs maintain high levels of *MDK* (Fig. 2c,e). By comparison, *PTN* was widely expressed in most types of retinal cells, and was significantly down-regulated by MG and MGPCs in damaged retinas (Fig. 2c,e). We queried expression of putative receptors for *MDK* and *PTN*, including *PTPRZ1, CSPG5* and Syndecan 4 (*SDC4*). Although *SDC4* was expressed in scattered retina cells, *SDC4* was low in resting MG and was up-regulated across MG at 24hrs after NMDA-treatment (Fig. 2d,e). *CSPG5* was expressed at high levels in resting MG, and was down-regulated in activated MG at 24hrs after NMDA and in MGPCs, and remained elevated in activated MG at 48 and 72hrs after NMDA (Fig. 2d,e). *PTPRZ1* was not detected in MG, but was expressed at high levels in NIRG cells and in scattered amacrine and bipolar cells (Fig. 2d). *CSPG5, SDC4, ITGB1*, and *PTN* were dynamically expressed by different retinal neurons and NIRG cells in NMDA-damaged retinas (Supplemental Fig. 2a-e), suggesting that MDK may influence NIRG cells and neurons following an insult.

Analysis of MG and MGPCs in different pseudotime states revealed a branched trajectory with resting MG, proliferating MGPCs, and activated MG from 72hr after NMDA-treatment largely confined to different branches and states (Supplemental Fig. 3a-d). The expression of *MDK* across pseudotime positively correlates with a transition toward an MGPC-phenotype and up-regulation of progenitor markers, such as *CDK1*,

and inversely correlated to resting glial phenotypes with significant down-regulation of glial markers such as *GLUL* (Supplemental Fig. 3a-d). By comparison, levels of *PTN* were decreased across pseudotime, with the largest decrease in *PTN* in activated MG compared to resting MG (Supplemental Fig. 3a-d). Similar to expression patterns of *CDK1*, patterns of expression of *SDC4* are significantly elevated in pseudotime state 4 populated by activated MG and proliferating MGPCs (Supplemental Fig. 3a-d).

When comparing MG and MGPCs from 48hrs after NMDA with and without FGF2 and insulin, the relative levels of *MDK* and *PTN* were significantly decreased (Fig. 2f-i). UMAP plots revealed distinct clustering of MG and MGPCs from retinas from 48hrs NMDA alone and 48hrs NMDA plus FGF2 and insulin (Fig. 2f-i). Similarly, levels of *GLUL, RLBP1* and *CSPG5* were significantly decreased by FGF2 and insulin in damaged retinas in both MG and MGPCs (Fig. 2f-I; Supplemental Fig. 3e-g). By contrast, levels of *CDK1* and *TOP2A* were significantly increased by FGF2 and insulin in MGPCs in damaged retinas (Supplemental Fig. 3e-g). Collectively, these findings suggest expression levels of *PTN* reflects a resting glial phenotype and levels are decreased by damage and further decreased by FGF2 and insulin, whereas expression levels of *MDK* corresponds with acutely activated glia or maturing glia, which is strongly induced by damage, but decreased by FGF2 and insulin in damaged retinas.

MDK, neuroprotection and glial reactivity in damaged retinas

The large, significant up-regulation of *MDK* by MG in NMDA-treated retinas suggests that this growth factor is involved in the responses of retinal cells to acute damage. To determine whether MDK influences retinal cells we probed for the activation of different cell-signaling pathways following a single intraocular injection of recombinant MDK or PTN. Four hours after delivery of MDK we found a significant up-regulation of cFOS and pS6 specifically in MG (Fig. 3a-e), suggesting activation of the mTor-pathway. In addition, amacrine cells appeared to significantly up-regulate cFOS and NIRG cells up-regulated pS6 in response to MDK (Fig. 3a-e). To test whether cell signaling was influenced by PP2A-inhibitors, we co-applied fostriecin and calyculin A with MDK. We found that fostriecin and calyculin A significantly reduced levels of pS6 in MDK-treated MG (Fig. 3f,g), where cfos activation was unaffected and independent of

PP2A inhibition (data not shown). We failed to find up-regulation of pERK1/2, p38 MAPK, pCREB, pSmad1/5/8, pStat3, and nuclear smad2/3 following intravitreal delivery of MDK (not shown). We failed to detect changes in cell signaling in response to intraocular injections of PTN (not shown). Despite distinct activation of cFOS and mTor in MG from a single dose of MDK, four consecutive daily intraocular injections of MDK or PTN had no significant effect upon MG reactivity or formation of proliferating MGPCs (not shown).

Intravitreal injections of MDK after NMDA-treatment had no significant effect upon glial reactivity or proliferation of MGPCs, NIRG cells or microglia (not shown). Concurrent administration lacked significant effects because endogenous levels of MDK were very high and MDK-mediated cell-signaling may have been saturated. By comparison, injection of MDK prior to NMDA-treatment significantly reduced the numbers of proliferating MGPCs that accumulated EdU or were immunolabeled for pHisH3 (Fig. 4a-d). Similarly, there was a significant reduction in the number $Sox2^{+}/Nkx2.2^{+}$ NIRG cells that accumulated in NMDA-damaged retinas (Fig. 4e,f). To determine whether microglial reactivity was influenced by MDK we measured the area and intensity sum for CD45 immunofluorescence, which is increased in reactive microglia (Fischer et al., 2014). Both the area and the intensity of CD45-immunofluorescence was decreased in response to MDK (Fig. 4g,h). We failed to detect a significant MDK-mediated change in well-established read-outs of different cell-signaling pathways including pS6, pCREB, p38 MAPK, pERK1/2, or pStat3 at later time points after damage (data not shown).

Levels of retinal damage and cell death positively correlate to numbers of proliferating MGPCs (Fischer and Reh, 2001; Fischer and Reh, 2003). Thus, it is possible that reduced numbers of proliferating MGPCs resulted from less cell death with MDK pre-treatment. Using the TUNEL method to labeling dying cells, we found that the administration of MDK before NMDA-damage significantly reduced numbers of dying cells (Fig. 4i,j). Decreased numbers of dying cells were observed at both 24h and 72h after NMDA-treatment with MDK pre-treatment. To complement the cell death studies, we probed for long-term survival of inner retinal neurons. Although there was no change

in numbers of AP2α$^+$ amacrine cells, there was a significant increase in numbers of calretinin$^+$ cells in retinas treated with MDK (Fig. 4k,i).

PTN was significantly down-regulated in MG following NMDA-treatment (Fig. 2). Despite the administration of high doses (1µg/dose) of PTN, intravitreal delivery of PTN with NMDA had no measurable effects on the formation of MGPCs, the reactivity and proliferation of microglia, and accumulation of NIRG cells (data not shown). Although these experiments were conducted using recombinant human PTN, there is high conservation between chick, mouse and human PTN (92% & 93% respectively).

Inhibition of MDK-signaling in damaged retinas

MDK-signaling is often upregulated in tissues with proliferating cells, such as tumors, and this proliferation can be suppressed by inhibition of MDK-signaling (Hao et al., 2013; Takei et al., 2006). Since levels of *MDK* were markedly increased in MG in damaged retinas, we tested whether inhibition of MDK-signaling influenced the formation of proliferating MGPCs. We applied a MDK-expression inhibitor (MDKi), which downregulates protein expression in a dose dependent manner (Masui et al., 2016). However, application of MDKi after NMDA-treatment failed to influence MG, NIRG cells, or microglia (data not shown). Alternatively, we applied a PTPRZ inhibitor SCB4380 that targets the intracellular domain of the receptor (Fujikawa et al., 2016). However, this inhibitor failed to influence MG, NIRG cells or microglia when applied after NMDA-treatment (not shown). It is likely that MDKi and SCB4380 had poor cellular permeability or species specificity and these drugs failed to adequately diffuse into the retina and mediate cellular changes.

We next applied an inhibitor of MDK-signaling, sodium orthovanadate (Na_3VO_4) that suppresses the activity of tyrosine phosphatase activity including PTPRZ1 (Qi et al., 2001), which was predominantly expressed by NIRG cells, amacrine cells, and some bipolar cells (Fig. 2c). Application of Na_3VO_4 with and after NMDA significantly reduced numbers of proliferating MGPCs (Fig. 5a,b). In addition, treatment with Na_3VO_4 significantly increased numbers of NIRG cells in the IPL (Fig. 5c,d) and increased numbers of dying cells (Fig. 5e,f). Despite this increase in retinal damage, proliferation

of MGPCs was reduced in response to Na_3VO_4 after NMDA-induced damage (Fig. 5a,b).

We next examined the specificity of Na_3VO_4, by testing whether Na_3VO_4 blocked the effects of MDK when applied with NMDA-treatment. Comparison across treatment groups (NMDA alone, NMDA + Na_3VO_4, NMDA + MDK, and NMDA + Na_3VO_4 + MDK) revealed a significant decrease in MGPCs in eyes treated with Na_3VO_4 and MDK alone (Fig. 5g,h). With the combination of MDK and Na_3VO_4 there was a significant increase in proliferating MGPCs relative to treatment with MDK or Na_3VO_4 alone (Fig. 5h). However, this level was not increased relative to levels seen with NMDA alone (Fig. 5h). In addition, the combination of MDK and Na_3VO_4 resulted in no significant difference in numbers of TUNEL$^+$ dying cells compared to NMDA alone (Fig 5i). These findings suggest that the effects of MDK and Na_3VO_4 upon proliferating MGPCs and numbers of dying neurons are mediated by overlapping cellular targets.

Putative MDK receptors, signal transducers and MGPC formation

MDK has been found to bind and signal through Integrin-Beta 1 (ITGB1) (Muramatsu et al., 2004). ITGB1 signaling through secondary messengers Integrin linked kinase (ILK), p21 activated kinase 1 (PAK1), cell division factor 42 (CDC42), protein phosphatase 2a (PP2A, gene: *PPP2CA*), and Git/Cat-1 regulate cytoskeleton remodeling, migration, and cellular proliferation (Bagrodia and Cerione, 1999; Ivaska et al., 1999; Kawachi et al., 2001; Kim et al., 2004; Martin et al., 2016; Mulrooney et al., 2000) (see Fig. 12). *PAK1* has been implicated as a cell cycle regulator that is downstream of MDK and PTN signaling (Kawachi et al., 2001). PAKs are components of the mitogen activated protein kinase (MAPK) pathway and are believed to regulate small GTP-binding proteins (CDC42 and RAC) (Bagrodia and Cerione, 1999; Frisch, 2000) (see Fig. 12).

By probing scRNA-seq libraries we found that *PAK1* was widely expressed at relatively high levels in resting MG, and levels were significantly reduced in MG at different times after NMDA, and further reduced in MGPCs (Fig. 6a,b). Similarly, levels of *PPP2CA*, *CDC42, GIT1* and *ILK* were expressed at relatively high levels in resting MG, but were widely expressed at reduced levels in MGPCs and activated MG in

damaged retinas (Fig. 6a,b). In addition, *PPP2CA*, *CDC42, GIT1* and *ILK* were expressed by different types of retinal neurons, NIRG cells and oligodendrocytes (Fig. 6a). We found that MG expressed *ITGB1* and other integrin isoforms, including *ITGA1, ITGA2, ITGA3* and *ITGA6* (Fig. 6a,b). In general, integrins were expressed at high levels in scattered resting MG, whereas levels were reduced, but more widely expressed among activated MG, and further reduced in MGPCs (Fig. 6a,b).

We next tested how PAK1 and PP2A influence the formation of MGPCs in NMDA-damaged retinas. MDK-signaling is known to be modulated by the second messenger PAK1 which is up-regulated in proliferating cancerous cells (Kumar et al., 2006). IPA3 is an isoform-specific allosteric inhibitor of PAK1 which prevents auto-phosphorylation (Deacon et al., 2008). Administration of IPA3 with NMDA significantly decreased numbers of proliferating MGPCs (Fig. 6c,d). By contrast, IPA3 had no significant effect upon the proliferation and accumulation of NIRG cells or microglia (Supplemental Fig. 4). Unlike Na_3VO_4, IPA3 had no impact on numbers of TUNEL$^+$ cells compared to those seen in retinas treated with NMDA alone (Supplemental Fig. 4). Since *PAK1* expression was most prevalent in resting MG and decreased after NMDA damage, we tested whether application of IPA3 prior to NMDA influenced glial cells and neuronal survival. We found that IPA3 prior to NMDA resulted in a significant decrease in proliferating MGPCs (Fig. 6e), whereas there was no significant difference in numbers of dying cells or proliferation of microglia and NIRG cells (Supplemental Fig. 4). Similar to the effects of IPA3, two different inhibitors to PP2A, fostriecin and calyculin A, significantly decreased numbers of proliferating MGPCs in NMDA-damaged retinas (Fig. 6f-h). Fostriecin and calyculin A had relatively little effect upon the accumulation, reactivity, cell death and proliferation of NIRG cells and microglia, with the exception of a small but significant decrease in proliferating microglia with calyculin A-treatment compared to controls (Supplemental Fig. 4). Collectively, these findings suggest that inhibition of signal-transducers of MDK-signaling suppresses the formation of MGPCs.

MDK **in retinas treated with insulin and FGF2**

In the postnatal chick retina, the formation of proliferating MGPCs can be induced by consecutive daily injections of Fibroblast growth factor 2 (FGF2) and insulin

in the absence of neuronal damage (Fischer et al., 2002b). Eyes were treated with two or three consecutive daily doses of FGF2 and insulin and retinas were processed to generate scRNA-seq libraries. Cells were clustered based on their gene expression in UMAP plots and colored by their library of origin (Fig. 7a,b). MG glia were identified based on collective expression of *VIM, GLUL* and *SLC1A3* and MGPCs were identified based on expression of *TOP2A, NESTIN, CCNB2* and *CDK1* for MGPCs (Supplemental Fig. 5a,b). Resting MG from saline-treated retinas formed a cluster distinct from MG from retinas treated with two- and three-doses of FGF2+insulin based on unique patterns of gene expression (Fig. 7b; Supplemental Fig. 5a,b). Additionally, MG treated with 2 versus 3 doses of insulin and FGF2 were sufficiently dissimilar to follow different trajectories of gene expression in pseudotime analysis (Supplemental Fig. 5c,d).

Similar to patterns of express in NMDA-damaged retinas, there was a significant increase in *MDK* with growth factor-treatment as demonstrated by patterns of expression in UMAP and violin plots, and pseudotime analyses (Fig. 7c-e; Supplemental Fig. 5d-f). By comparison, levels of *PTN* were significantly decreased in MG following treatment with insulin and FGF2 (Fig. 7c,e; Supplemental Fig. 5d-f). Similarly, levels of *PAK1* were decreased in activated MG and MGPCs in response to growth factor treatment (Fig. 7d,e; Supplemental Fig. 5e,f). *CSPG5* was widely expressed at high levels in scattered resting MG, and was significantly reduced in MG and MGPCs following treatment with insulin and FGF2 (Fig. 7d,e; Supplemental Fig. 5e, f). *ITGB1* expression was scattered in resting MG, and decreased slightly in MG and MGPCs treated with insulin and FGF2 (Fig. 7d,e; Supplemental Fig. 5e,f). In sum, treatment with FGF2 and insulin in the absence of retina damage influenced patterns of expression for MDK-related genes similar to those seen in NMDA-damaged retinas.

We next isolated MG, aggregated and normalized scRNA-seq data from saline-, NMDA-, FGF2+insulin- and NMDA/FGF2+insulin-treated retinas to directly compare levels of *MDK*, *PTN* and related factors. UMAP plots revealed distinct clustering of MG from control retinas and MG from 24hrs after NMDA-treatment, whereas MG from retinas at 48 and 72hrs after NMDA and from retinas treated with insulin and FGF2 formed a large cluster with distinct regions (Fig. 8a-e). UMAP and Dot plots revealed distinct patterns of expression of genes associated with resting MG, de-differentiating

MG, activated MG and proliferating MGPCs (Fig. 8c-e). Different zones, representing MGPCs in different phases of the cell cycle were comprised of cells from different times after NMDA-treatment and FGF2+insulin-treatment (Fig. 8e). Expression of *MDK* was most widespread and significantly up-regulated in MG in damaged retinas and MGPCs compared to MG from retinas treated with insulin and FGF2 (Fig. 8f). Compared to levels seen in resting MG, levels of *PTN* were reduced in activated MG from damaged retinas and MGPCs, and levels were further decreased in MG from normal and damaged retinas that were treated with insulin and FGF2 (Fig. 8f); similar patterns of expression were seen for *PAK1, CSPG5, ITGB1, PPP2CA* and *CDC42*. By contrast, levels of *SDC4* were highest and most widespread in MG at 24hrs after NMDA-treatment and were relatively reduced in all other groups of MG and MGPCs (Fig. 8f). Collectively, these findings indicate that damaged-induced changes of *MDK*, *PTN* and related factors in MG are very dramatic, and these changes in relative expression levels in MG are dampened by insulin and FGF2 whether applied to undamaged or damaged retinas.

MDK and MGPCs in undamaged retinas.

In the absence of damage, in retinas treated with FGF2 and insulin, we tested whether MDK influences MG and the formation of MGPCs. MDK was administered two days before and with three consecutive daily doses of FGF2 and insulin (Fig. 9). MDK-treatment had no significant influence upon the formation of proliferating MGPCs or the accumulation of NIRG cells (Fig. 9a,b,c). We next tested whether inhibition of PAK1 with IPA3 influenced glial cells in retinas treated with FGF2 and insulin. IPA3-treatment had no significant influence upon the formation of proliferating MGPCs, NIRG cells or microglia (Fig. 9d-g), but did have a small, but significant, inhibitory effect upon the accumulation of NIRG cells (Fig. 9h). We next tested whether inhibition of PTPRZ with Na_3VO_4 influenced the glial cells in retinas treated with FGF2 and insulin. There was no significant difference in numbers of proliferating MGPCs following 3 days of treatment with insulin and FGF2 with Na_3VO_4 (Fig. 9i). Similarly, MDKi inhibitor had no effect upon the formation of proliferating MGPCs (not shown). However, there was an increase in the total number of NIRG cells in the retina in response to Na_3VO_4 treatment (Fig. 9j-k).

The reactivity and accumulation of microglia were unaffected by the Na_3VO_4 or IPA3 (data not shown).

***Mdk*, *Ptn* and MDK-receptors in damaged mouse retinas**

We next sought to assess the expression of *Mdk* and related factors in normal and NMDA-damaged mouse retinas. Comparison of the different responses of glial cells across species can indicate important factors that confer the potential of MG to reprogram into MGPCs (Hoang et al., 2019). UMAP analysis of cells from control and NMDA-damage mouse retinas revealed discrete clusters of different cell types (Fig. 10a). Neuronal cells from control and damaged retinas were clustered together, regardless of time after NMDA-treatment (Fig. 10a). By contrast, resting MG, which included MG from 48 and 72 hrs after NMDA, and activated MG from 3, 6, 12 and 24 hours after treated were spatially separated in UMAP plots (Fig. 10a,b). Pseudotime analysis placed resting MG (control and some MG from 48 and 72 hrs after treatment) to the left, MG from 3 and 6 hrs after treatment to the far right, and MG from 12 and 24 hrs bridging the middle (Supplemental Fig. 6a-d). Unlike chick MG, mouse MG rapidly downregulate *Mdk* in response to damage and this downregulation is maintained through 72 hrs after treatment (Fig. 10c,d). Similar to MG in the chick, *Ptn* was rapidly and significantly down-regulated at 3hrs, and further down-regulated at 6hrs, and sparsely expressed at 12-48hrs (Fig. 10c,d). Levels of *Pak1* were low in resting MG, and elevated in MG only at 3hrs after NMDA-treatment (Fig. 10c,d). Similar to chick MG, *Cspg5* was significantly decreased in activated MG in damaged retinas (Fig. 10c,d). By contrast, there were significant increases in levels of *Sdc4* and *Itgb1* in MG in damaged retinas (Fig. 10c,d; Supplemental Fig. 6e-g). We further analyzed the responses of MG in damaged retinas at 48hrs after NMDA ± treatment with insulin and FGF2, which is known to stimulate proliferation of MG (Karl et al., 2008). Treatment with FGF2 and insulin in damaged retinas significantly reduced levels of *Glul*, whereas levels of *Vim* and *Gfap* were significantly increased (Supplemental Fig. 6h-j). By comparison, levels of *Mdk* and *Sdc4* were significantly increased in MG in retinas treated with NMDA+FGF2/insulin, whereas levels of *Ptn*, *Cspg5* and *Itgb1* were unchanged (Supplemental Fig. 6h-j).

We next investigated the activation of different cell-signaling pathways in retinal cells in response to intravitreal delivery of MDK. We failed to detect activation of NFkB, pStat3, pSmad1/5/8, pCREB, p38 MAPK or pERK1/2 (not shown). However, in response to a single injection of MDK, we found a selective and significant up-regulation of cFOS and pS6 in MG (Fig. 11a-e), similar to that observed in chick retina. Other types of retinal cells did not appear to respond to MDK with up-regulation of cFOS or pS6. We next tested whether intraocular injections of MDK combined with NMDA-induced damage influences the proliferation of MG in the mouse retina. Consistent with previous reports (Karl et al., 2008), there were very few proliferating MG in NMDA-damaged retinas (Fig. 11f,h). By contrast, application of MDK with NMDA resulted in a small, but significant increase in numbers of proliferating MG (Fig. 11f-h).

Discussion:

In the chick retina, we find that dynamic expression of *MDK* during retinal development and in mature retinas following injury or growth factor-treatment. High levels of *MDK* expression were selectively and rapidly induced in MG following damage or treatment with insulin and FGF2, with larger increases in expression seen in damaged tissues. Addition of exogenous MDK before damage was neuroprotective and resulted in decreased numbers of proliferating MGPCs. Antagonism of MDK-signaling reduced numbers of proliferating MGPCs and stimulated the accumulation of NIRG cells and increased numbers of dying cells. Na_3VO_4 and PAK1 antagonist had differential effects on NIRG cells and cell death that were context dependent. In contrast to the findings in chick, we find that *Mdk* is down-regulated by MG in damaged mouse retinas. In both chick and mouse retinas, exogenous MDK selectively induces mTOR-signaling and expression of cFOS in MG.

PTN signaling in the retina

PTN and MDK are in the same family of growth factors and are both dynamically expressed in the developing, damaged, and growth factor treated retinas. Although treatment with MDK had varying effects on MG, microglia, NIRGs, and neurons, PTN administration failed to illicit detectable effects upon retinal cells. Levels of *PTN* are high

in resting MG and down-regulated in response to neuronal damage or treatment with insulin and FGF2. In principle, PTN acts at the same receptors as MDK, but expression of receptor isoforms may underlie the different cellular responses to MDK and PTN. PTN has preferred binding-affinity for SDC4 and ITGB3, whereas MDK has preferred binding-affinity for SDC3 and ITGB1 (Muramatsu et al., 2004; Raulo et al., 1994; Xu et al., 2014), which are expression by bipolar cells and MG.

PTN and MDK may induce different biological effects on the same receptors. For instance, data suggests that there may be differential receptor activity between PTN and MDK on the PTPRz receptor. Binding of PTN to PTPRz induces oligomerization of the receptor that reduces phosphatase activity (Fukada et al., 2006). Conversely, MDK promotes embryonic neuronal survival in a PTPRz receptor complex, which is inhibited by Na_3VO_4 (Sakaguchi et al., 2003). Although we failed to detect PTN-mediated effects upon retinal cells, PTN may serve other important biological roles in retinal hometostasis, glial phenotype/functions or neuroprotection in other models of retinal damage.

Receptor expression and cells responding to MDK

The effects of MDK on retinal glia has not been studied in mammals or birds. In acutely damaged chick retina, MG are capable of forming numerous proliferating progenitor cells (MGPCs), but few of the progeny differentiate into neurons (Fischer and Reh, 2001; Fischer and Reh, 2002). The reprogramming of MG into MGPCs can be induced by FGF2 and insulin in the absence of damage through MAPK signaling (Fischer and Reh, 2002; Fischer et al., 2002a; Fischer et al., 2002b). Similarly, IGF1, BMP, retinoic acid, sonic hedgehog, Wnt, and Jak/Stat agonists have been observed to enhance the formation of MGPCs (Fischer et al., 2009a; Gallina et al., 2015; Todd and Fischer, 2015; Todd et al., 2016; Todd et al., 2017; Todd et al., 2018). Consistent across the different signaling pathways that drive the formation of proliferating MGPCs is the up-regulation of cFOS and necessity for mTor-signaling in reprogramming MG (Zelinka et al., 2016). Previous reports have provided many examples of MDK activating cell-signaling pathways that drive proliferation (Reiff et al., 2011; Winkler and Yao, 2014). Accordingly, we propose that MDK-mediated cell-signaling that results in

activation of cFOS and mTOR contributes to the network of pathways that drive the formation of proliferating MGPCs in the chick retinas.

Patterns of expression for receptors suggests than glial cells and inner retinal neurons are targets of MDK and PTN. In MG the predominant receptor is *ITGB1*, whereas NIRGs cells express *PTPRZ1*, and amacrine and bipolar cells express a combination of *PTPRZ1* and *SDC4*. The mechanism by which ITGB1 and PTPRZ influence cell cycle and differentiation are distinctly different. PTPRZ promotes stem cell characteristics and ligand binding inhibits this phosphatase function (Fujikawa et al., 2016; Fukada et al., 2006; Kuboyama et al., 2015). Signal transduction through ITGB1 influences cytoskeleton remodeling that is associated with cell migration and proliferation (Muramatsu et al., 2004). ITGB1 can activate or inhibit secondary messengers depending on tyrosine phosphorylation (Kim et al., 2004; Mulrooney et al., 2000; Song et al., 2014). Ligand binding to ITGB1 initiates tyrosine phosphorylation of intracellular domains, and integrin linked kinases (ILKs) activate PP2A and cell cycle kinases, such as CDC42 (Ivaska et al., 1999; Ivaska et al., 2002). The transcriptional profiles of individual retinal cell types suggest that MDK and PTN likely have autocrine and paracrine actions that are dynamically regulated in damaged retinas and manifested through MG, and dynamic regulation of mRNA is strongly correlated with changes in protein levels and function (Liu et al., 2016).

MDK-signaling in MG

Application of MDK prior to NMDA-induced damage decreased numbers of proliferating MGPCs and decreased numbers of dying cells. Levels of retinal damage positively correlate to the proliferative response of MG (Fischer and Reh, 2001; Fischer et al., 2004). We propose that the neuroprotective effects of MDK secondarily influenced the proliferative of MGPCs. It is possible that the addition of MDK to damaged retinas failed to influence MGPCs because of “ceiling effects” wherein (i) ligand/receptor interactions are saturated, (ii) the activity of secondary messengers are saturated, or (iii) the massive up-regulation of MDK by MG is not directly involved in driving the formation of proliferating MGPCs.

Phosphatase inhibitor Na_3VO_4 suppressed the formation of MGPCs and increased cell death, and these effects where blocked by addition of MDK. Inhibition of intracellular phosphatases, such as PP2A that are commonly associated with ITGB1 receptors, increasing the upstream activation may be attributed to restoring MG responses to damage. Inhibition of Git/Cat-1/PAK1-signaling is associated with ITGB1-mediated cytoskeleton remodeling during migration and proliferation (Martin et al., 2016; Muramatsu et al., 2004). Consistent with these observations, we found that inhibition of PAK1 and PP2A effectively suppressed the formation of MGPCs in damaged retinas. Further studies are required to identify changes in phosphorylation and expression that are down-stream of PP2A activity.

MDK and cell-signaling inhibitors failed to have significant impacts upon MG and microglia in retinas treated with insulin and FGF2. Similar to NMDA-treatment, we see significant changes in expression levels of *MDK*, *PTN*, *PAK1* and *CSPG5*, suggesting that MDK-signaling is active in undamaged retinas treated with insulin and FGF2 (see Fig. 7). However, direct comparison of relative expression levels of *MDK* and related genes across all treatment groups indicated that: (i) although *MDK* is up-regulated with insulin and FGF2, levels are much less than those seen with NMDA alone, (ii) *SDC4* is modestly induced in MG by insulin and FGF2, and (iii) levels of *PAK1*, *CSPG5, ITGB1, PPP2CA* and *CDC4* are further down-regulated by insulin and FGF2 compared to levels seen with NMDA-treatment. The diminished levels of MDK-receptors and signal transducers in MG treated with insulin and FGF2, compared to levels in MG treated with NMDA, may underlie the absence of effects of exogenous MDK and inhibitors. This suggests that MDK and down-stream signaling are not required for the formation of MGPCs in retinas treated with insulin+FGF2. Alternatively, the cell-signaling pathways that are activated by MDK are the same as those activated by insulin+FGF2 and there is no net gain in second messenger activation in MG by combining these factors. This is unique because many signaling pathways that have been implicated in regulating the formation of MGPCs in the chick retina are active following NMDA-induced damage and treatment with insulin and FGF2. These pathways include MAPK (Fischer et al., 2009a; Fischer et al., 2009b), mTOR (Zelinka et al., 2016), Notch (Ghai et al., 2010; Hayes et al., 2007), Jak/Stat (Todd et al., 2016), Wnt/b-catenin (Gallina et al., 2015),

glucocorticoid (Gallina, 2015), Hedgehog (Todd and Fischer, 2015), BMP/SMAD (Todd et al., 2017), retinoic acid (Todd et al., 2018) and NFkB-signaling (Palazzo et al., 2020).

MDK signaling in NIRG cells

A well-established receptor of MDK is PTPRz (Maeda et al., 1999). PTPRz is a cell-surface receptor that acts as a protein tyrosine phosphatase and is known to promotes proliferation (Fujikawa et al., 2016). This receptor is activated by MDK (Sakaguchi et al., 2003), but is deactivated by the binding of PTN through dimerization and tyrosine phosphorylation (Kuboyama et al., 2015). NIRG cells predominantly express *PTPRZ1* and the accumulation of these cells in response to damage was decreased with MDK-treatment and increased by treatment with phosphatase inhibitor Na_3VO_4. The accumulation of NIRG cells may result, in part, from migration, as MDK has been associated with migration and process elongation in different cell types (Ichihara-Tanaka et al., 2006; Kuboyama et al., 2015; Qi et al., 2001). Given that nothing is currently known about the specific functions of NIRG cells, it is difficult to infer how activation/inhibition of MDK-signaling in these glia impacts the reprogramming of MG or function/survival of retinal neurons.

MDK and reprogramming of MG into MGPCs

There has been significant research understanding the cell-signaling pathways involved in the reprogramming of MG into proliferating MGPCs. IGF1, BMP, retinoic acid, HB-EGF, sonic hedgehog, Wnt, and CNTF are known to enhance the formation of MGPCs (Fischer et al., 2009a; Fischer et al., 2009b; Gallina et al., 2015; Todd and Fischer, 2015; Todd et al., 2016; Todd et al., 2017; Todd et al., 2018). The roles of these different pathways are similar in chick and zebrafish models of retinal regeneration, despite different capacities for neurogenesis (Goldman, 2014; Wan and Goldman, 2016). MDK has been implicated as an important factor to drive de-differentiation MG into proliferating progenitor cells (Calinescu et al., 2009; Luo et al., 2012; Nagashima et al., 2019). In the chick model, different inhibitors to PAK1, PP2A and PTPRZ1 had relatively modest impacts on the formation of MGPCs. Although exogenous MDK likely added nothing to already saturated levels in damaged retinas,

MDK alone was not sufficient to induce the formation of MGPCs in the absence of damage when levels of MDK were low. These findings suggest that MDK signaling is not a primary signaling component to drive the formation of MGPCs in chick, unlike the key role for MDK seen in zebrafish (Gramage et al., 2015; Nagashima et al., 2019). In the chick, our findings suggests that MDK has pleiotropic roles and serves to both minimize neuronal cell death after damage and regulate the accumulation of NIRG cells. By comparison to effects seen in chick MG, MDK stimulated mTor-signaling and cFos expression in mouse MG and induced a modest increase in numbers of proliferating MG in damaged retinas. The neurogenic potential of these few proliferating MG remains to be determined.

Conclusions:

MDK and *PTN* are highly expressed by maturing MG in embryonic retinas, and *MDK* is down-regulated while *PTN* remains highly expressed by resting MG in the retinas of hatched chicks. In mature mouse retinas, *PTN* had similar patterns of expression, whereas *MDK* showed patterns of expression opposite to those seen in chick MG. When MG are stimulated by growth factors or neuronal damage in the chick model, *MDK* is robustly up-regulated whereas *PTN* is down-regulated. Injections of MDK had significant effects upon proliferating glia, formation of MGPCs, and glial reactivity, whereas we failed to detect cellular responses to exogenous PTN. Elevated MDK demonstrated survival-promoting effects upon neurons, and subsequently suppressed MGPC formation. Inhibiting factors associated with the ITGB1 signaling complex dampened MGPC formation and phosphatase inhibitor Na_3VO_4 over-rode the effects of MDK upon neuronal survival and MGPC formation. This effect was limited to damaged retinas, whereas in retinas treated with insulin+FGF2 there may be a convergence or over-lap of cell-signaling pathways activated by MDK and insulin+FGF2. In determining its effectiveness at driving dedifferentiation and proliferation of MG in mouse models of excitotoxic damage, only a small but significant increase in MGPCs was observed. Overall, the up regulation of *MDK* is among the largest increases in gene expression detected in MG stimulate by damage or growth

factors, implying significant multifactorial functions in the context of development, reprogramming, and response to tissue damage.

Author contributions: WAC – experimental design, execution of experiments, collection of data, data analysis, construction of figures and writing the manuscript. MF and IP – execution of experiments and collection of data. TH and SB – preparation of scRNA-seq libraries. AJF – experimental design, data analysis, construction of figures and writing the manuscript.

Competing Interests: The authors have no competing interests to declare.

Data availability: RNA-Seq data are deposited in GEO (GSE135406)
Chick scRNA-Seq data can be queried at
https://proteinpaint.stjude.org/F/2019.retina.scRNA.html.

References:

Bagrodia, S. and Cerione, R. A. (1999). PAK to the future. *Trends Cell Biol.* **9**, 350–355.

Bernardos, R. L., Barthel, L. K., Meyers, J. R. and Raymond, P. A. (2007). Late-stage neuronal progenitors in the retina are radial Muller glia that function as retinal stem cells. *J Neurosci* **27**, 7028–40.

Butler, A., Hoffman, P., Smibert, P., Papalexi, E. and Satija, R. (2018). Integrating single-cell transcriptomic data across different conditions, technologies, and species. *Nat. Biotechnol.* **36**, 411–420.

Calinescu, A.-A., Vihtelic, T. S., Hyde, D. R. and Hitchcock, P. F. (2009). The Cellular Expression of Midkine-a and Midkine-b During Retinal Development and Photoreceptor Regeneration in Zebrafish. *J. Comp. Neurol.* **514**, 1–10.

Dai, L.-C., Yao, X., Wang, X., Niu, S.-Q., Zhou, L.-F., Fu, F.-F., Yang, S.-X. and Ping, J.-L. (2009). In vitro and in vivo suppression of hepatocellular carcinoma growth by midkine-antisense oligonucleotide-loaded nanoparticles. *World J. Gastroenterol. WJG* **15**, 1966–1972.

Deacon, S. W., Beeser, A., Fukui, J. A., Rennefahrt, U. E. E., Myers, C., Chernoff, J. and Peterson, J. R. (2008). An isoform-selective, small-molecule inhibitor targets the autoregulatory mechanism of p21-activated kinase. *Chem. Biol.* **15**, 322–331.

Fabri, L., Maruta, H., Muramatsu, H., Muramatsu, T., Simpson, R. J., Burgess, A. W. and Nice, E. C. (1993). Structural characterisation of native and recombinant forms of the neurotrophic cytokine MK. *J. Chromatogr.* **646**, 213–225.

Fausett, B. V. and Goldman, D. (2006). A role for alpha1 tubulin-expressing Muller glia in regeneration of the injured zebrafish retina. *J Neurosci* **26**, 6303–13.

Fausett, B. V., Gumerson, J. D. and Goldman, D. (2008). The proneural basic helix-loop-helix gene ascl1a is required for retina regeneration. *J. Neurosci. Off. J. Soc. Neurosci.* **28**, 1109–1117.

Fischer, A. J. and Reh, T. A. (2001). Müller glia are a potential source of neural regeneration in the postnatal chicken retina. *Nat. Neurosci.* **4**, 247–252.

Fischer, A. J. and Reh, T. A. (2002). Exogenous growth factors stimulate the regeneration of ganglion cells in the chicken retina. *Dev Biol* **251**, 367–79.

Fischer, A. J. and Reh, T. A. (2003). Potential of Muller glia to become neurogenic retinal progenitor cells. *Glia* **43**, 70–6.

Fischer, A. J., Seltner, R. L. P., Poon, J. and Stell, W. K. (1998). Immunocytochemical characterization of quisqualic acid- and N-methyl-D-aspartate-induced excitotoxicity in the retina of chicks. *J. Comp. Neurol.* **393**, 1–15.

Fischer, A. J., Dierks, B. D. and Reh, T. A. (2002a). Exogenous growth factors induce the production of ganglion cells at the retinal margin. *Development* **129**, 2283–91.

Fischer, A. J., McGuire, C. R., Dierks, B. D. and Reh, T. A. (2002b). Insulin and Fibroblast Growth Factor 2 Activate a Neurogenic Program in Müller Glia of the Chicken Retina. *J. Neurosci.* **22**, 9387–9398.

Fischer, A. J., Foster, S., Scott, M. A. and Sherwood, P. (2008). The transient expression of LIM-domain transcription factors is coincident with the delayed maturation of photoreceptors in the chicken retina. *J. Comp. Neurol.* **506**, 584–603.

Fischer, A. J., Scott, M. A., Ritchey, E. R. and Sherwood, P. (2009a). Mitogen-activated protein kinase-signaling regulates the ability of Müller glia to proliferate and protect retinal neurons against excitotoxicity. *Glia* **57**, 1538–1552.

Fischer, A. J., Scott, M. A. and Tuten, W. (2009b). Mitogen-activated protein kinase-signaling stimulates Muller glia to proliferate in acutely damaged chicken retina. *Glia* **57**, 166–81.

Fischer, A. J., Zelinka, C., Gallina, D., Scott, M. A. and Todd, L. (2014). Reactive microglia and macrophage facilitate the formation of Müller glia-derived retinal progenitors. *Glia* **62**, 1608–1628.

Frisch, S. M. (2000). cAMP takes control. *Nat. Cell Biol.* **2**, E167–E168.

Fujikawa, A., Nagahira, A., Sugawara, H., Ishii, K., Imajo, S., Matsumoto, M., Kuboyama, K., Suzuki, R., Tanga, N., Noda, M., et al. (2016). Small-molecule inhibition of PTPRZ reduces tumor growth in a rat model of glioblastoma. *Sci. Rep.* **6**, 20473.

Fukada, M., Fujikawa, A., Chow, J. P. H., Ikematsu, S., Sakuma, S. and Noda, M. (2006). Protein tyrosine phosphatase receptor type Z is inactivated by ligand-induced oligomerization. *FEBS Lett.* **580**, 4051–4056.

Gallina, D. Z., C. P. Cebulla, C. M. Fischer, A. J. (2015). Activation of glucocorticoid receptors in Müller glia is protective to retinal neurons and suppresses microglial reactivity. *Exp Neurol* **273**, 114–125.

Gallina, D., Palazzo, I., Steffenson, L., Todd, L. and Fischer, A. J. (2015). Wnt/betacatenin-signaling and the formation of Muller glia-derived progenitors in the chick retina. *Dev Neurobiol*.

Ghai, K., Zelinka, C. and Fischer, A. J. (2009). Serotonin released from amacrine neurons is scavenged and degraded in bipolar neurons in the retina. *J Neurochem* **111**, 1–14.

Ghai, K., Zelinka, C. and Fischer, A. J. (2010). Notch signaling influences neuroprotective and proliferative properties of mature Muller glia. *J Neurosci* **30**, 3101–12.

Goldman, D. (2014). Müller glial cell reprogramming and retina regeneration. *Nat. Rev. Neurosci.* **15**, 431–442.

Gramage, E., Li, J. and Hitchcock, P. (2014). The expression and function of midkine in the vertebrate retina. *Br J Pharmacol* **171**, 913–23.

Gramage, E., D'Cruz, T., Taylor, S., Thummel, R. and Hitchcock, P. F. (2015). Midkine-a Protein Localization in the Developing and Adult Retina of the Zebrafish and Its Function During Photoreceptor Regeneration. *PLoS ONE* **10**,.

Hao, H., Maeda, Y., Fukazawa, T., Yamatsuji, T., Takaoka, M., Bao, X.-H., Matsuoka, J., Okui, T., Shimo, T., Takigawa, N., et al. (2013). Inhibition of the Growth Factor MDK/Midkine by a Novel Small Molecule Compound to Treat Non-Small Cell Lung Cancer. *PLOS ONE* **8**, e71093.

Hayes, S., Nelson, B. R., Buckingham, B. and Reh, T. A. (2007). Notch signaling regulates regeneration in the avian retina. *Dev Biol* **312**, 300–11.

Hitchcock, P. F. and Raymond, P. A. (1992). Retinal regeneration. *Trends Neurosci* **15**, 103–8.

Hoang, T., Wang, J., Boyd, P., Wang, F., Santiago, C., Jiang, L., Lahne, M., Todd, L. J., Saez, C., Yoo, S., et al. (2019). Cross-species transcriptomic and epigenomic analysis reveals key regulators of injury response and neuronal regeneration in vertebrate retinas. *bioRxiv* 717876.

Ichihara-Tanaka, K., Oohira, A., Rumsby, M. and Muramatsu, T. (2006). Neuroglycan C Is a Novel Midkine Receptor Involved in Process Elongation of Oligodendroglial Precursor-like Cells. *J. Biol. Chem.* **281**, 30857–30864.

Ivaska, J., Reunanen, H., Westermarck, J., Koivisto, L., Kähäri, V.-M. and Heino, J. (1999). Integrin α2β1 Mediates Isoform-Specific Activation of p38 and Upregulation of Collagen Gene Transcription by a Mechanism Involving the α2 Cytoplasmic Tail. *J. Cell Biol.* **147**, 401–416.

Ivaska, J., Nissinen, L., Immonen, N., Eriksson, J. E., Kähäri, V.-M. and Heino, J. (2002). Integrin α2β1 Promotes Activation of Protein Phosphatase 2A and Dephosphorylation of Akt and Glycogen Synthase Kinase 3β. *Mol. Cell. Biol.* **22**, 1352–1359.

Iwasaki, W., Nagata, K., Hatanaka, H., Inui, T., Kimura, T., Muramatsu, T., Yoshida, K., Tasumi, M. and Inagaki, F. (1997). Solution structure of midkine, a new heparin-binding growth factor. *EMBO J.* **16**, 6936–6946.

Jochheim-Richter, A., Rüdrich, U., Koczan, D., Hillemann, T., Tewes, S., Petry, M., Kispert, A., Sharma, A. D., Attaran, F., Manns, M. P., et al. (2006). Gene expression analysis identifies novel genes participating in early murine liver development and adult liver regeneration. *Differentiation* **74**, 167–173.

Kang, H. C., Kim, I.-J., Park, J.-H., Shin, Y., Ku, J.-L., Jung, M. S., Yoo, B. C., Kim, H. K. and Park, J.-G. (2004). Identification of Genes with Differential Expression in Acquired Drug-Resistant Gastric Cancer Cells Using High-Density Oligonucleotide Microarrays. *Clin. Cancer Res.* **10**, 272–284.

Karl, M. O., Hayes, S., Nelson, B. R., Tan, K., Buckingham, B. and Reh, T. A. (2008). Stimulation of neural regeneration in the mouse retina. *Proc Natl Acad Sci U A* **105**, 19508–13.

Kawachi, H., Fujikawa, A., Maeda, N. and Noda, M. (2001). Identification of GIT1/Cat-1 as a substrate molecule of protein tyrosine phosphatase ζ/β by the yeast substrate-trapping system. *Proc. Natl. Acad. Sci. U. S. A.* **98**, 6593–6598.

Kikuchi-Horie, K., Kawakami, E., Kamata, M., Wada, M., Hu, J.-G., Nakagawa, H., Ohara, K., Watabe, K. and Oyanagi, K. (2004). Distinctive expression of midkine in the repair period of rat brain during neurogenesis: Immunohistochemical and immunoelectron microscopic observations. *J. Neurosci. Res.* **75**, 678–687.

Kilpeläinen, I., Kaksonen, M., Kinnunen, §‖ Tarja, Avikainen, H., Fath, M., Linhardt, R. J., Raulo, E. and Rauvala, H. (2000). Heparin-binding Growth-associated Molecule Contains Two Heparin-binding β-Sheet Domains That Are Homologous to the Thrombospondin Type I Repeat. *J. Biol. Chem.* **275**, 13564–13570.

Kim, S.-M., Kwon, M. S., Park, C. S., Choi, K.-R., Chun, J.-S., Ahn, J. and Song, W. K. (2004). Modulation of Thr Phosphorylation of Integrin β1 during Muscle Differentiation. *J. Biol. Chem.* **279**, 7082–7090.

Kojima, T., Katsumi, A., Yamazaki, T., Muramatsu, T., Nagasaka, T., Ohsumi, K. and Saito, H. (1996). Human Ryudocan from Endothelium-like Cells Binds Basic Fibroblast Growth Factor, Midkine, and Tissue Factor Pathway Inhibitor. *J. Biol. Chem.* **271**, 5914–5920.

Kuboyama, K., Fujikawa, A., Suzuki, R. and Noda, M. (2015). Inactivation of Protein Tyrosine Phosphatase Receptor Type Z by Pleiotrophin Promotes Remyelination through Activation of Differentiation of Oligodendrocyte Precursor Cells. *J. Neurosci.* **35**, 12162–12171.

Kumar, R., Gururaj, A. E. and Barnes, C. J. (2006). p21-activated kinases in cancer. *Nat. Rev. Cancer* **6**, 459.

Kurosawa, N., Chen, G.-Y., Kadomatsu, K., Ikematsu, S., Sakuma, S. and Muramatsu, T. (2001). Glypican-2 binds to midkine: The role of glypican-2 in neuronal cell adhesion and neurite outgrowth. *Glycoconj. J.* **18**, 499–507.

Liu, Y., Beyer, A. and Aebersold, R. (2016). On the Dependency of Cellular Protein Levels on mRNA Abundance. *Cell* **165**, 535–550.

Luo, J., Uribe, R. A., Hayton, S., Calinescu, A.-A., Gross, J. M. and Hitchcock, P. F. (2012). Midkine-A functions upstream of Id2a to regulate cell cycle kinetics in the developing vertebrate retina. *Neural Develop.* **7**, 33.

Maeda, N., Ichihara-Tanaka, K., Kimura, T., Kadomatsu, K., Muramatsu, T. and Noda, M. (1999). A Receptor-like Protein-tyrosine Phosphatase PTPζ/RPTPβ Binds a Heparin-binding Growth Factor Midkine INVOLVEMENT OF ARGININE 78 OF MIDKINE IN THE HIGH AFFINITY BINDING TO PTPζ. *J. Biol. Chem.* **274**, 12474–12479.

Martin, K., Pritchett, J., Llewellyn, J., Mullan, A. F., Athwal, V. S., Dobie, R., Harvey, E., Zeef, L., Farrow, S., Streuli, C., et al. (2016). PAK proteins and YAP-1 signalling downstream of integrin beta-1 in myofibroblasts promote liver fibrosis. *Nat. Commun.* **7**, 1–11.

Mashima, T., Sato, S., Sugimoto, Y., Tsuruo, T. and Seimiya, H. (2009). Promotion of glioma cell survival by acyl-CoA synthetase 5 under extracellular acidosis conditions. *Oncogene* **28**, 9–19.

Masui, M., Okui, T., Shimo, T., Takabatake, K., Fukazawa, T., Matsumoto, K., Kurio, N., Ibaragi, S., Naomoto, Y., Nagatsuka, H., et al. (2016). Novel Midkine Inhibitor iMDK Inhibits Tumor Growth and Angiogenesis in Oral Squamous Cell Carcinoma. *Anticancer Res.* **36**, 2775–2781.

Mirkin, B. L., Clark, S., Zheng, X., Chu, F., White, B. D., Greene, M. and Rebbaa, A. (2005). Identification of midkine as a mediator for intercellular transfer of drug resistance. *Oncogene* **24**, 4965.

Mitsiadis, T. A., Salmivirta, M., Muramatsu, T., Muramatsu, H., Rauvala, H., Lehtonen, E., Jalkanen, M. and Thesleff, I. (1995). Expression of the heparin-binding cytokines, midkine (MK) and HB-GAM (pleiotrophin) is associated with epithelial-mesenchymal interactions during fetal development and organogenesis. *Development* **121**, 37–51.

Miyashiro, M., Kadomatsu, K., Ogata, N., Yamamoto, C., Takahashi, K., Uyama, M., Muramatsu, H. and Muramatsu, T. (1998). Midkine expression in transient retinal ischemia in the rat. *Curr. Eye Res.* **17**, 9–13.

Mulrooney, J., Foley, K., Vineberg, S., Barreuther, M. and Grabel, L. (2000). Phosphorylation of the β1 Integrin Cytoplasmic Domain: Toward an Understanding of Function and Mechanism. *Exp. Cell Res.* **258**, 332–341.

Muramatsu, T. (2002). Midkine and pleiotrophin: two related proteins involved in development, survival, inflammation and tumorigenesis. *J Biochem* **132**, 359–71.

Muramatsu, H., Zou, K., Sakaguchi, N., Ikematsu, S., Sakuma, S. and Muramatsu, T. (2000). LDL Receptor-Related Protein as a Component of the Midkine Receptor. *Biochem. Biophys. Res. Commun.* **270**, 936–941.

Muramatsu, H., Zou, P., Suzuki, H., Oda, Y., Chen, G.-Y., Sakaguchi, N., Sakuma, S., Maeda, N., Noda, M., Takada, Y., et al. (2004). α4β1- and α6β1-integrins are functional receptors for midkine, a heparin-binding growth factor. *J. Cell Sci.* **117**, 5405–5415.

Nagashima, M., D'Cruz, T. S., Danku, A. E., Hesse, D., Sifuentes, C., Raymond, P. A. and Hitchcock, P. F. (2019). Midkine-a is required for cell cycle progression of Müller glia glia during neuronal regeneration in the vertebrate retina. *J. Neurosci.*

Nakanishi, T., Kadomatsu, K., Okamoto, T., Ichihara-Tanaka, K., Kojima, T., Saito, H., Tomoda, Y. and Muramatsu, T. (1997). Expression of Syndecan-1 and -3 during Embryogenesis of the Central Nervous System in Relation to Binding with Midkine. *J. Biochem. (Tokyo)* **121**, 197–205.

Obama, H., Biro, S., Tashiro, T., Tsutsui, J., Ozawa, M., Yoshida, H., Tanaka, H. and Muramatsu, T. (1998). Myocardial infarction induces expression of midkine, a heparin-binding growth factor with reparative activity. *Anticancer Res.* **18**, 145–152.

Ooto, S., Akagi, T., Kageyama, R., Akita, J., Mandai, M., Honda, Y. and Takahashi, M. (2004). Potential for neural regeneration after neurotoxic injury in the adult mammalian retina. *Proc Natl Acad Sci U A* **101**, 13654–9.

Palazzo, I., Deistler, K., Hoang, T. V., Blackshaw, S. and Fischer, A. J. (2020). NF-κB signaling regulates the formation of proliferating Müller glia-derived progenitor cells in the avian retina. *Development*.

Pollak, J., Wilken, M. S., Ueki, Y., Cox, K. E., Sullivan, J. M., Taylor, R. J., Levine, E. M. and Reh, T. A. (2013). ASCL1 reprograms mouse Müller glia into neurogenic retinal progenitors. *Dev. Camb. Engl.* **140**, 2619–2631.

Qi, M., Ikematsu, S., Maeda, N., Ichihara-Tanaka, K., Sakuma, S., Noda, M., Muramatsu, T. and Kadomatsu, K. (2001). Haptotactic Migration Induced by Midkine INVOLVEMENT OF PROTEIN-TYROSINE PHOSPHATASE ζ, MITOGEN-ACTIVATED PROTEIN KINASE, AND PHOSPHATIDYLINOSITOL 3-KINASE. *J. Biol. Chem.* **276**, 15868–15875.

Qiu, X., Hill, A., Packer, J., Lin, D., Ma, Y.-A. and Trapnell, C. (2017a). Single-cell mRNA quantification and differential analysis with Census. *Nat. Methods* **14**, 309–315.

Qiu, X., Mao, Q., Tang, Y., Wang, L., Chawla, R., Pliner, H. A. and Trapnell, C. (2017b). Reversed graph embedding resolves complex single-cell trajectories. *Nat. Methods* **14**, 979–982.

Raulo, E., Chernousov, M. A., Carey, D. J., Nolo, R. and Rauvala, H. (1994). Isolation of a neuronal cell surface receptor of heparin binding growth-associated molecule (HB-GAM). Identification as N-syndecan (syndecan-3). *J. Biol. Chem.* **269**, 12999–13004.

Raymond, P. A. (1991). Retinal regeneration in teleost fish. *Ciba Found Symp* **160**, 171–86; discussion 186-91.

Reiff, T., Huber, L., Kramer, M., Delattre, O., Janoueix-Lerosey, I. and Rohrer, H. (2011). Midkine and Alk signaling in sympathetic neuron proliferation and neuroblastoma predisposition. *Development* **138**, 4699–4708.

Reynolds, P. R., Mucenski, M. L., Cras, T. D. L., Nichols, W. C. and Whitsett, J. A. (2004). Midkine Is Regulated by Hypoxia and Causes Pulmonary Vascular Remodeling. *J. Biol. Chem.* **279**, 37124–37132.

Sakaguchi, N., Muramatsu, H., Ichihara-Tanaka, K., Maeda, N., Noda, M., Yamamoto, T., Michikawa, M., Ikematsu, S., Sakuma, S. and Muramatsu, T. (2003). Receptor-type protein tyrosine phosphatase ζ as a component of the signaling receptor complex for midkine-dependent survival of embryonic neurons. *Neurosci. Res.* **45**, 219–224.

Sakakima, H., Kamizono, T., Matsuda, F., Izumo, K., Ijiri, K. and Yoshida, Y. (2006). Midkine and its receptor in regenerating rat skeletal muscle after bupivacaine injection. *Acta Histochem.* **108**, 357–364.

Salama, R. H. M., Muramatsu, H., Zou, P., Okayama, M. and Muramatsu, T. (2006). Midkine, a heparin-binding growth factor, produced by the host enhances metastasis of Lewis lung carcinoma cells. *Cancer Lett.* **233**, 16–20.

Satija, R., Farrell, J. A., Gennert, D., Schier, A. F. and Regev, A. (2015). Spatial reconstruction of single-cell gene expression data. *Nat Biotechnol* **33**, 495–502.

Shen, X., Xi, G., Wai, C. and Clemmons, D. R. (2015). The Coordinate Cellular Response to Insulin-like Growth Factor-I (IGF-I) and Insulin-like Growth Factor-binding Protein-2 (IGFBP-2) Is Regulated through Vimentin Binding to Receptor Tyrosine Phosphatase β (RPTPβ). *J. Biol. Chem.* **290**, 11578–11590.

Song, J., Zhang, J., Wang, J., Cao, Z., Wang, J., Guo, X. and Dong, W. (2014). β1 integrin modulates tumor growth and apoptosis of human colorectal cancer. *Oncol. Rep.* **32**, 302–308.

Stanke, J., Moose, H. E., El-Hodiri, H. M. and Fischer, A. J. (2010). Comparative study of Pax2 expression in glial cells in the retina and optic nerve of birds and mammals. *J Comp Neurol* **518**, 2316–33.

Takei, Y., Kadomatsu, K., Matsuo, S., Itoh, H., Nakazawa, K., Kubota, S. and Muramatsu, T. (2001). Antisense Oligodeoxynucleotide Targeted to Midkine, a Heparin-binding Growth Factor, Suppresses Tumorigenicity of Mouse Rectal Carcinoma Cells. *Cancer Res.* **61**, 8486–8491.

Takei, Y., Kadomatsu, K., Goto, T. and Muramatsu, T. (2006). Combinational antitumor effect of siRNA against midkine and paclitaxel on growth of human prostate cancer xenografts. *Cancer* **107**, 864–873.

Thillai, K., Lam, H., Sarker, D. and Wells, C. M. (2016). Deciphering the link between PI3K and PAK: An opportunity to target key pathways in pancreatic cancer? *Oncotarget* **8**, 14173–14191.

Todd, L. and Fischer, A. J. (2015). Hedgehog signaling stimulates the formation of proliferating Müller glia-derived progenitor cells in the chick retina. *Dev. Camb. Engl.* **142**, 2610–2622.

Todd, L., Squires, N., Suarez, L. and Fischer, A. J. (2016). Jak/Stat signaling regulates the proliferation and neurogenic potential of Müller glia-derived progenitor cells in the avian retina. *Sci. Rep.* **6**,.

Todd, L., Palazzo, I., Squires, N., Mendonca, N. and Fischer, A. J. (2017). BMP- and TGFβ-signaling regulate the formation of Müller glia-derived progenitor cells in the avian retina. *Glia* **65**, 1640–1655.

Todd, L., Suarez, L., Quinn, C. and Fischer, A. J. (2018). Retinoic Acid-Signaling Regulates the Proliferative and Neurogenic Capacity of Müller Glia-Derived Progenitor Cells in the Avian Retina. *STEM CELLS* **36**, 392–405.

Trapnell, C., Roberts, A., Goff, L., Pertea, G., Kim, D., Kelley, D. R., Pimentel, H., Salzberg, S. L., Rinn, J. L. and Pachter, L. (2012). Differential gene and transcript expression analysis of RNA-seq experiments with TopHat and Cufflinks. *Nat Protoc* **7**, 562–78.

Tsutsui, J., Uehara, K., Kadomatsu, K., Matsubara, S. and Muramatsu, T. (1991). A new family of heparin-binding factors: Strong conservation of midkine (MK) sequences between the human and the mouse. *Biochem. Biophys. Res. Commun.* **176**, 792–797.

Tsutsui, J., Kadomatsu, K., Matsubara, S., Nakagawara, A., Hamanoue, M., Takao, S., Shimazu, H., Ohi, Y. and Muramatsu, T. (1993). A New Family of Heparin-binding Growth/Differentiation Factors: Increased Midkine Expression in Wilms' Tumor and Other Human Carcinomas. *Cancer Res.* **53**, 1281–1285.

Ueki, Y., Wilken, M. S., Cox, K. E., Chipman, L., Jorstad, N., Sternhagen, K., Simic, M., Ullom, K., Nakafuku, M. and Reh, T. A. (2015). Transgenic expression of the proneural transcription factor Ascl1 in Müller glia stimulates retinal regeneration in young mice. *Proc. Natl. Acad. Sci.* **112**, 13717–13722.

Unoki, K., Ohba, N., Arimura, H., Muramatsu, H. and Muramatsu, T. (1994). Rescue of photoreceptors from the damaging effects of constant light by midkine, a retinoic acid-responsive gene product. *Invest. Ophthalmol. Vis. Sci.* **35**, 4063–4068.

Van Rooijen, N. (1989). The liposome-mediated macrophage 'suicide' technique. *J. Immunol. Methods* **124**, 1–6.

van Rooijen, N. (1992). Liposome-mediated elimination of macrophages. *Res Immunol* **143**, 215–9.

Wan, J. and Goldman, D. (2016). Retina regeneration in zebrafish. *Curr. Opin. Genet. Dev.* **40**, 41–47.

Winkler, C. and Yao, S. (2014). The midkine family of growth factors: diverse roles in nervous system formation and maintenance. *Br. J. Pharmacol.* **171**, 905–912.

Xu, C., Zhu, S., Wu, M., Han, W. and Yu, Y. (2014). Functional Receptors and Intracellular Signal Pathways of Midkine (MK) and Pleiotrophin (PTN). *Biol. Pharm. Bull.* **37**, 511–520.

Zelinka, C. P., Scott, M. A., Volkov, L. and Fischer, A. J. (2012). The Reactivity, Distribution and Abundance of Non-Astrocytic Inner Retinal Glial (NIRG) Cells Are Regulated by Microglia, Acute Damage, and IGF1. *PLOS ONE* **7**, e44477.

Zelinka, C. P., Volkov, L., Goodman, Z. A., Todd, L., Palazzo, I., Bishop, W. A. and Fischer, A. J. (2016). mTor signaling is required for the formation of proliferating Müller glia-derived progenitor cells in the chick retina. *Dev. Camb. Engl.* **143**, 1859–1873.

Zou, K., Muramatsu, H., Ikematsu, S., Sakuma, S., Salama, R. H. M., Shinomura, T., Kimata, K. and Muramatsu, T. (2000). A heparin-binding growth factor, midkine, binds to a chondroitin sulfate proteoglycan, PG-M/versican. *Eur. J. Biochem.* **267**, 4046–4053.

1082

Figure legends:

Figure 1. Expression of *MDK*, *PTN* and *CSPG5* in maturing MG in embryonic chick retina. scRNA-seq was used to identify patterns of expression of *MDK*, *PTN* and putative receptor *CSPG5* among embryonic retinal cells at four stages of development (E5, E8, E12, E15). UMAP-ordered clusters of cells were identified by expression of hallmark genes (**a,b**). A heatmap of *MDK*, *PTN* and *CSPG5* illustrates expression profiles in different developing retinal cells (**c**). Each dot represents one cell and black dots indicate cells with 2 or more genes expressed. The upregulation of MDK and PTN in RPCs and maturing MG is illustrated with violin plot (**d**). The number on each violin indicates the percentage of expressing cells. The transition from RPC to mature MG is modelled with pseudotime ordering of cells with early RPCs to the far left and maturing MG to the right of the pseudotime trajectory (**e**). *MDK* and *PTN* are up-regulated in MG during maturation as illustrated by the pseudotime heatmap (**f**) and pseudotime plot (**g**). Significant difference (*$p<0.01$, **$p<0.0001$, ***$p<<0.0001$) was determined by using a Wilcox rank sum with Bonferoni correction. RPC – retinal progenitor cell, MG – Müller glia, iMG – immature Müller glia, mMG - mature Müller glia.

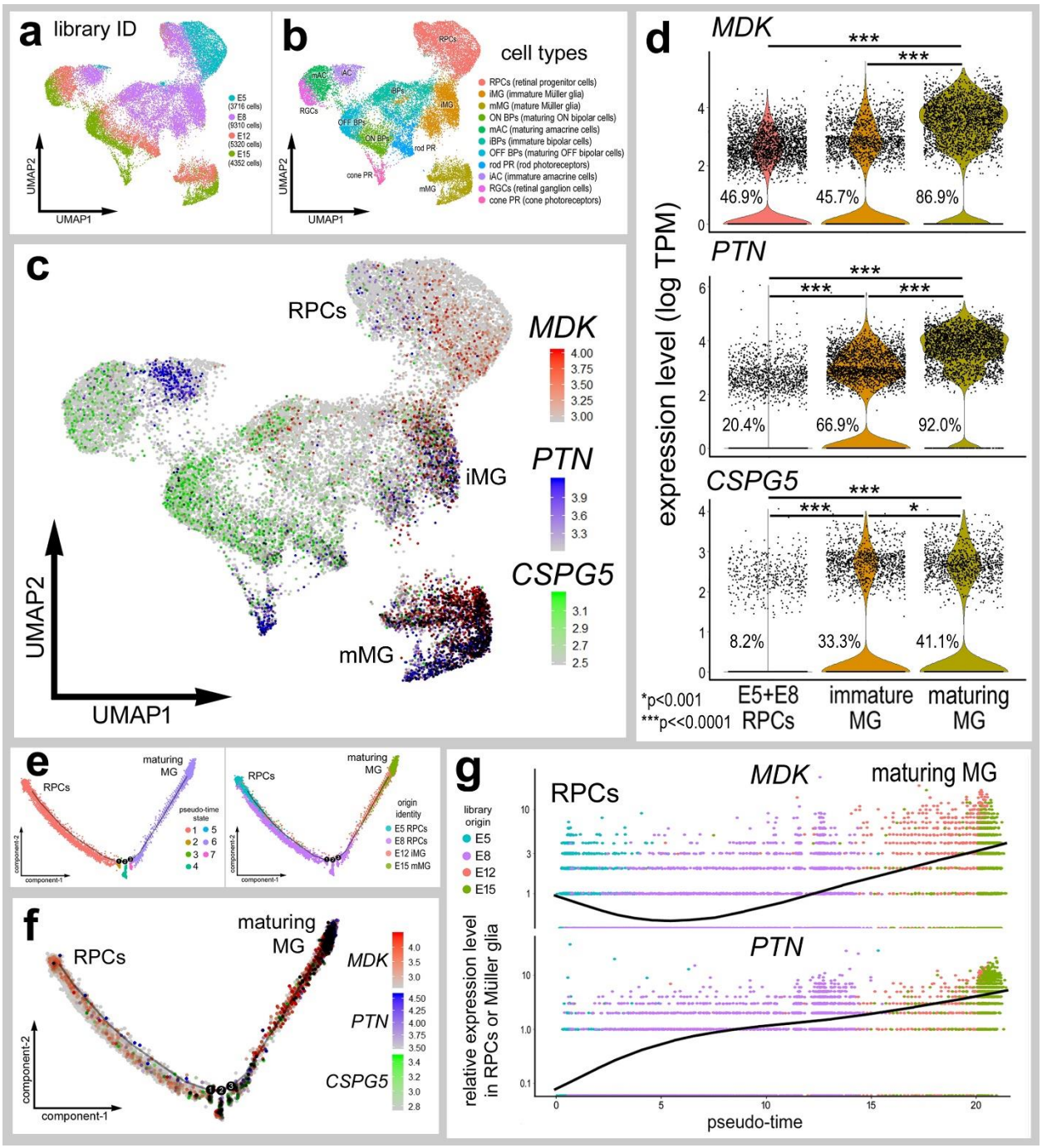
a
library ID
E5 (3716 cells)
E8 (9310 cells)
E12 (5320 cells)
E15 (4352 cells)
UMAP2
UMAP1
b
cell types
RPCs (retinal progenitor cells)
iMG (immature Müller glia)
mMG (mature Müller glia)
ON BPs (maturing ON bipolar cells)
mAC (maturing amacrine cells)
iBPs (immature bipolar cells)
OFF BPs (maturing OFF bipolar cells)
rod PR (rod photoreceptors)
iAC (immature amacrine cells)
RGCs (retinal ganglion cells)
cone PR (cone photoreceptors)
c
RPCs
iMG
mMG
MDK
PTN
CSPG5
d
MDK
PTN
CSPG5
expression level (log TPM)
46.9%
45.7%
86.9%
20.4%
66.9%
92.0%
8.2%
33.3%
41.1%
*p<0.001
***p<<0.0001
E5+E8 RPCs
immature MG
maturing MG
e
RPCs
maturing MG
pseudo-time state
origin identity
E5 RPCs
E8 RPCs
E12 iMG
E15 mMG
component-1
component-2
f
RPCs
maturing MG
MDK
PTN
CSPG5
component-1
component-2
g
library origin
E5
E8
E12
E15
RPCs
MDK
maturing MG
PTN
relative expression level in RPCs or Müller glia
pseudo-time

Figure 2. The expression profile of *MDK*, *PTN* and putative receptors in mature retinal cells and following acute injury. scRNA-seq was used to identify patterns of expression of MDK-related genes among acutely dissociated retinal cells with the data presented in UMAP plots (**a**-**d, f, g, h**) and violin plots (**e**,**i**). Control and treated scRNA-seq libraries were aggregated from 24hr, 48hr, and 72hr after NMDA-treatment (**a**). UMAP-ordered cells formed distinct clusters with MG and MGPCs forming distinct clusters (**b**). Expression heatmaps of *MDK*, *PTN*, and receptor genes *PTPRZ1*, *CSPG5*, and *SDC4* demonstrate patterns of expression in the retina, with black dots representing cells with 2 or more genes (**c,d**). In addition to NMDA, retinas were treated with insulin and FGF2 and expression levels of *MDK*, *PTN*, and *CSPG5* were assessed in MG and MGPCs (**f**-**i**). UMAP and violin plots illustrate relative levels of expression in MG and MGPCs treated with NMDA alone or NMDA plus insulin and FGF2 (**h,i**). Violin plots illustrate levels of gene expression and significant changes (*$p<0.1$, **$p<0.0001$, ***$p<<0.0001$) in levels were determined by using a Wilcox rank sum with Bonferroni correction. The number on each violin indicates the percentage of expressing cells.

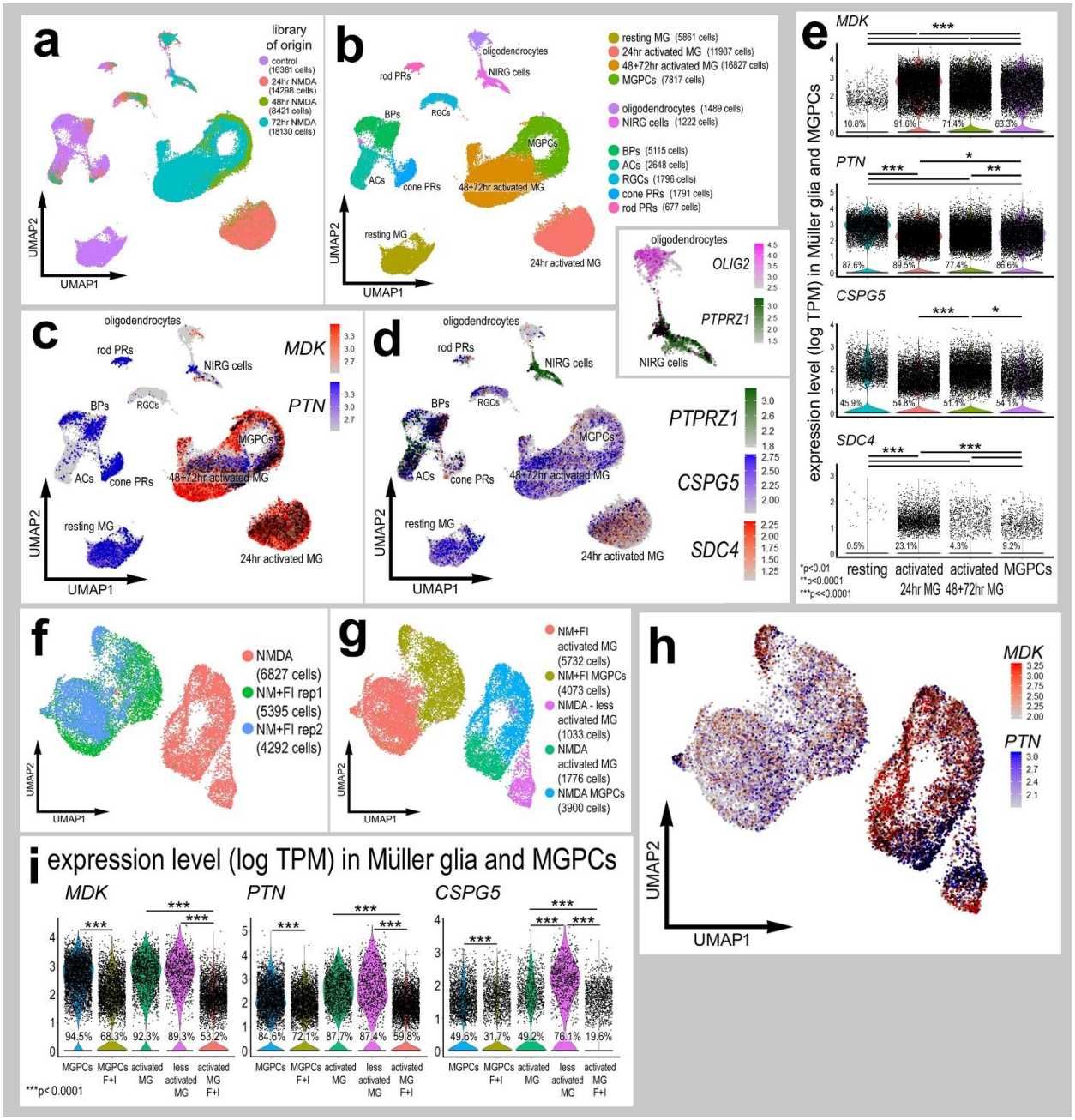
a
library of origin
control (16381 cells)
24hr NMDA (14296 cells)
48hr NMDA (8421 cells)
72hr NMDA (18130 cells)
UMAP2
UMAP1
b
resting MG (5861 cells)
24hr activated MG (11987 cells)
48+72hr activated MG (16827 cells)
MGPCs (7817 cells)
oligodendrocytes (1489 cells)
NIRG cells (1222 cells)
BPs (5115 cells)
ACs (2648 cells)
RGCs (1796 cells)
cone PRs (1791 cells)
rod PRs (677 cells)
oligodendrocytes
NIRG cells
rod PRs
BPs
RGCs
MGPCs
ACs
cone PRs
48+72hr activated MG
resting MG
24hr activated MG
OLIG2
PTPRZ1
c
MDK
PTN
d
PTPRZ1
CSPG5
SDC4
e
MDK
PTN
CSPG5
SDC4
expression level (log TPM) in Müller glia and MGPCs
resting
activated 24hr MG
activated 48+72hr MG
MGPCs
*p<0.01
**p<0.0001
***p<<0.0001
f
NMDA (6827 cells)
NM+FI rep1 (5395 cells)
NM+FI rep2 (4292 cells)
g
NM+FI activated MG (5732 cells)
NM+FI MGPCs (4073 cells)
NMDA - less activated MG (1033 cells)
NMDA activated MG (1776 cells)
NMDA MGPCs (3900 cells)
h
MDK
PTN
i expression level (log TPM) in Müller glia and MGPCs
MDK
PTN
CSPG5
MGPCs
MGPCs F+I
activated MG
less activated MG
activated MG F+I
***p< 0.0001

Figure 3. MDK activates cell-signaling in MG in the chick retina. A single intraocular injection of MDK was delivered and retinas were harvested 4 hours later. The histogram in **a** represents the mean percent change (±SD) in intensity sum for cFOS and pS6 immunofluorescence. Each dot represents one biological replicate retina. Significance of difference (**p<0.01, ***p<0.001) was determined by using a paired *t*-test. Sections of saline (control) and MDK-treated retinas were labeled with antibodies to cFOS (green; **b**,**c**), pS6 (green; **d**,**e**) and Sox2 (magenta; **c**,**e**). Arrows indicate the nuclei of MG, small double-arrows indicate the nuclei of amacrine cells, and hollow arrow-heads indicate the nuclei of presumptive NIRG cells. An identical paradigm with the addition of ITGB1 inhibitors fostriecin & calyculin measured changes in pS6 signaling in MG (**f**) and was quantified for intensity changes (**g**)**.** The calibration bar (50 µm) in panel **d** applies to **b** and **d**. Abbreviations: ONL – outer nuclear layer, INL – inner nuclear layer, IPL – inner plexiform layer, GCL – ganglion cell layer.

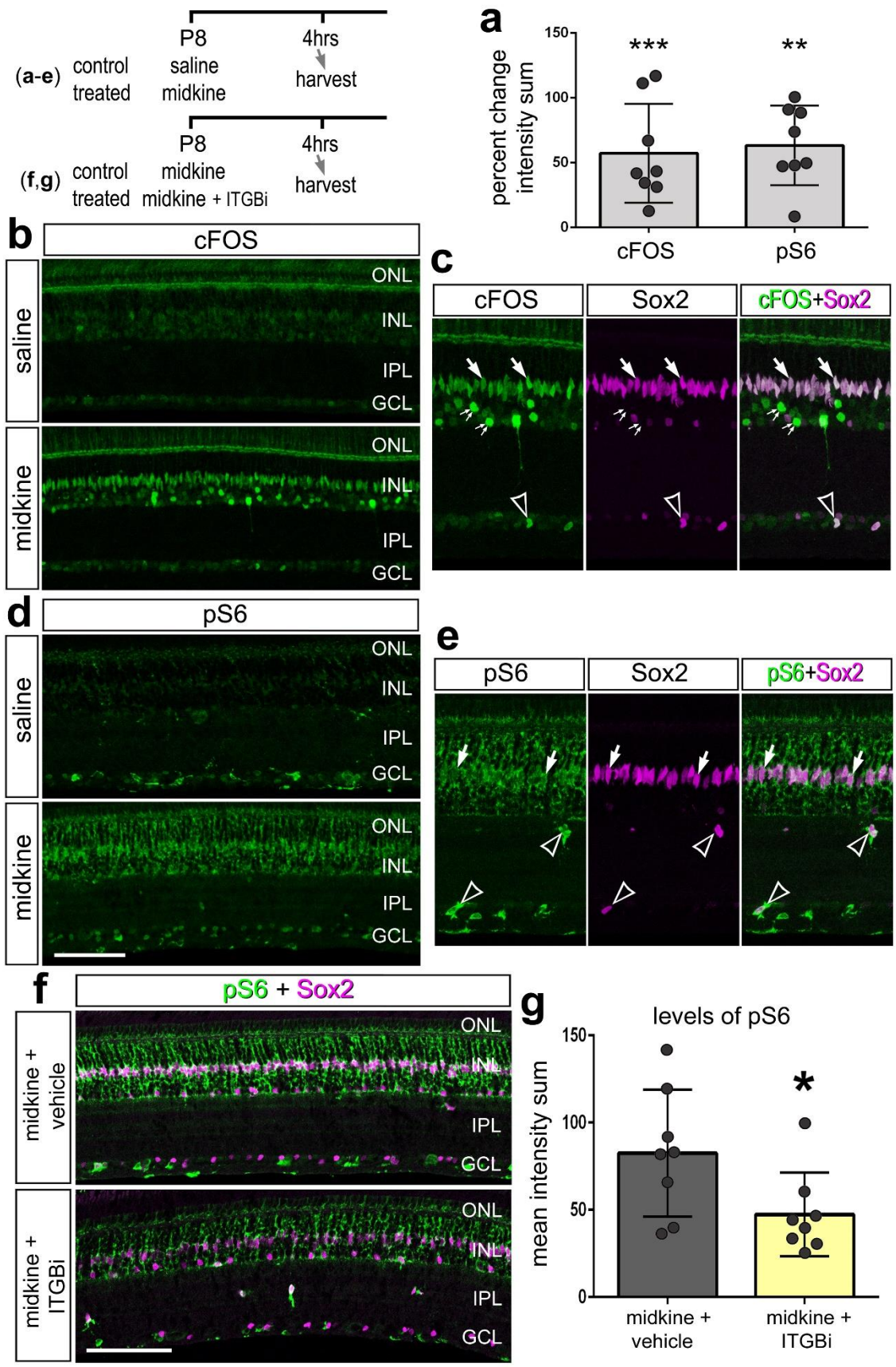
(a-e)
control
treated
P8
saline
midkine
4hrs
harvest
(f,g)
control
treated
P8
midkine
midkine + ITGBi
4hrs
harvest
a
percent change intensity sum
150
100
50
0
***
**
cFOS
pS6
b
cFOS
saline
midkine
ONL
INL
IPL
GCL
c
cFOS
Sox2
cFOS+Sox2
d
pS6
e
pS6
Sox2
pS6+Sox2
f
pS6 + Sox2
midkine + vehicle
midkine + ITGBi
g
levels of pS6
mean intensity sum
*
midkine + vehicle
midkine + ITGBi

1135

Figure 4. MDK treatment prior to NMDA reduces numbers of proliferating MGPCs, suppresses the accumulation of NIRG cells, and increases neuronal survival. Eyes were injected with MDK or saline at P6 and P7, and NMDA at P8. Some retinas were harvested at P9, whereas other eyes were injected at P10 with EdU and retinas harvested 4hrs later, 24hrs later at P11 or 10 days later at P20. Sections of the retina were labeled for EdU (red) and Sox9 (green; **a**), phospho-Histone H3 (pHisH3; magenta) and Sox2 (green; **c**), Nkx2.2 (**e**), CD45 (**g**), TUNEL (**i**), and AP2α (red) and Otx2 (green) or calretinin (red; **k**). Arrows indicate nuclei of proliferating MGPCs and hollow arrow-heads indicate TUNEL-positive cells. The histogram/scatter-plots **b**, **d, f, j** and **l** illustrate the mean number of labeled cells (±SD). The histogram in **h** represents the mean percent change (±SD) in density sum and area for CD45 immunofluorescence. Each dot represents one biological replicate. Significance of difference (*$p<0.01$) was determined by using a paired *t*-test. The calibration bars panels **a**, **c, e, g, i** and **k** represent 50 µm. Abbreviations: ONL – outer nuclear layer, INL – inner nuclear layer, IPL – inner plexiform layer, GCL – ganglion cell layer.

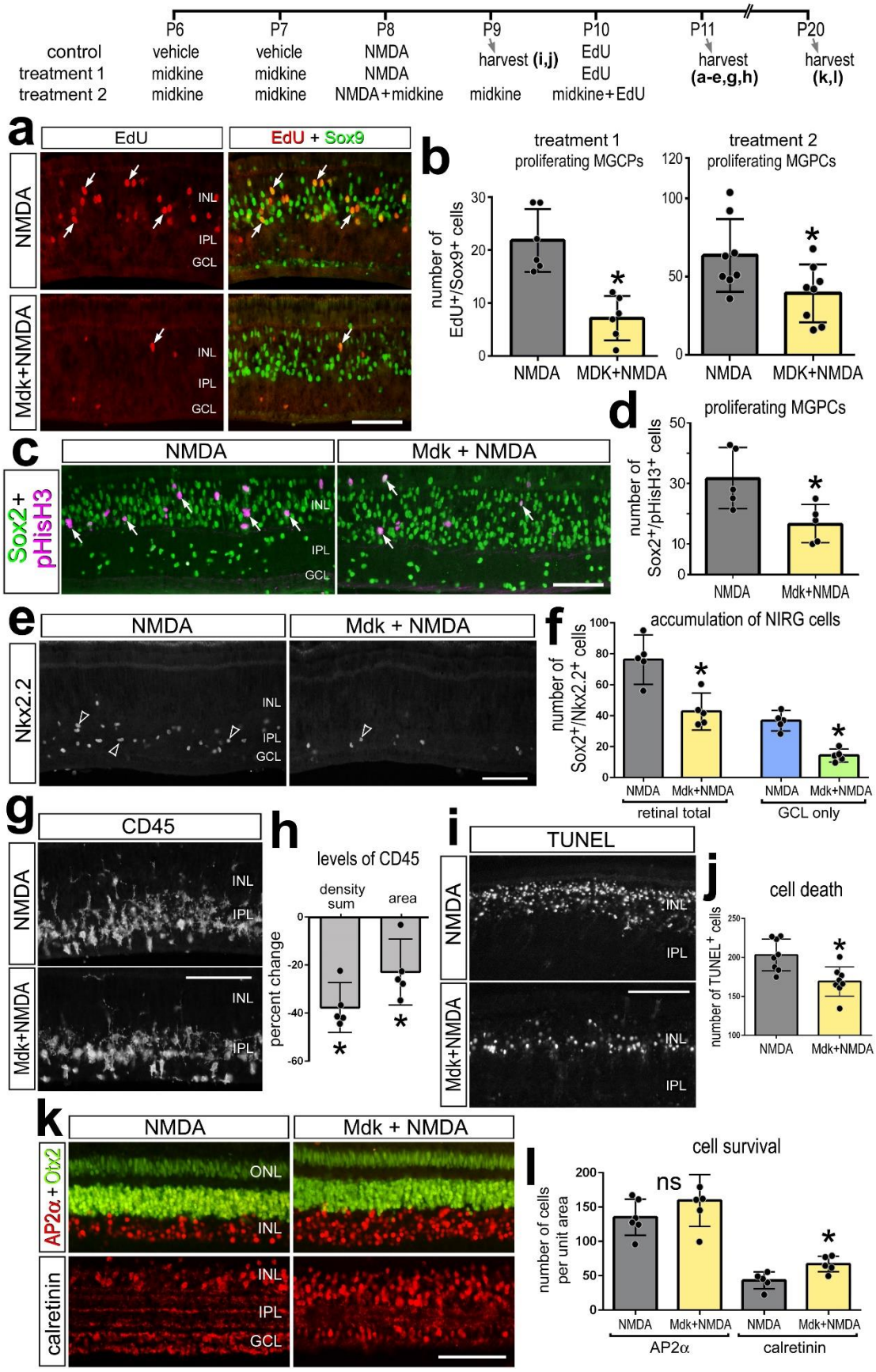
P6
P7
P8
P9
P10
P11
P20
control
treatment 1
treatment 2
vehicle
midkine
midkine
vehicle
midkine
midkine
NMDA
NMDA
NMDA+midkine
harvest (i,j)
midkine
EdU
EdU
midkine+EdU
harvest (a-e,g,h)
harvest (k,l)
a
EdU
EdU + Sox9
NMDA
Mdk+NMDA
INL
IPL
GCL
b
treatment 1
proliferating MGCPs
treatment 2
proliferating MGPCs
number of EdU+/Sox9+ cells
NMDA
MDK+NMDA
c
NMDA
Mdk + NMDA
Sox2+ pHisH3
d
proliferating MGPCs
number of Sox2+/pHisH3+ cells
e
Nkx2.2
f
accumulation of NIRG cells
number of Sox2+/Nkx2.2+ cells
retinal total
GCL only
g
CD45
h
levels of CD45
density sum
area
percent change
i
TUNEL
j
cell death
number of TUNEL+ cells
k
AP2α + Otx2
calretinin
ONL
l
cell survival
ns
number of cells per unit area
AP2α
calretinin

1152

Figure 5. Inhibition of PTPrz in NMDA-damaged retinas suppressed the formation of MGPCs, increases numbers of dying cells, and stimulates the accumulation of NIRG cells. Eyes were injected with NMDA and Na_3VO_4 inhibitor or vehicle at P8, inhibitor or vehicle at P9, EdU at P10, and retinas harvested at P11. Sections of the retina were labeled for EdU (red) and Sox9 (green; **a, g**), Nkx2.2 and Sox9 (green; **c**), or TUNEL (**e**). Arrows indicate nuclei of proliferating MGPCs (**a,g**) and hollow arrow-heads indicate NIRG cells (**c**). The histogram/scatter-plots in **b**, **d, f, h** and **i** illustrate the mean (±SD) number of labeled cells. Each dot represents one biological replicate. Significance of difference (*$p<0.05$) was determined by using a paired *t*-test. The calibration bars panels **a**, **c, e** and **g** represent 50 µm. Abbreviations: ONL – outer nuclear layer, INL – inner nuclear layer, IPL – inner plexiform layer, GCL – ganglion cell layer.

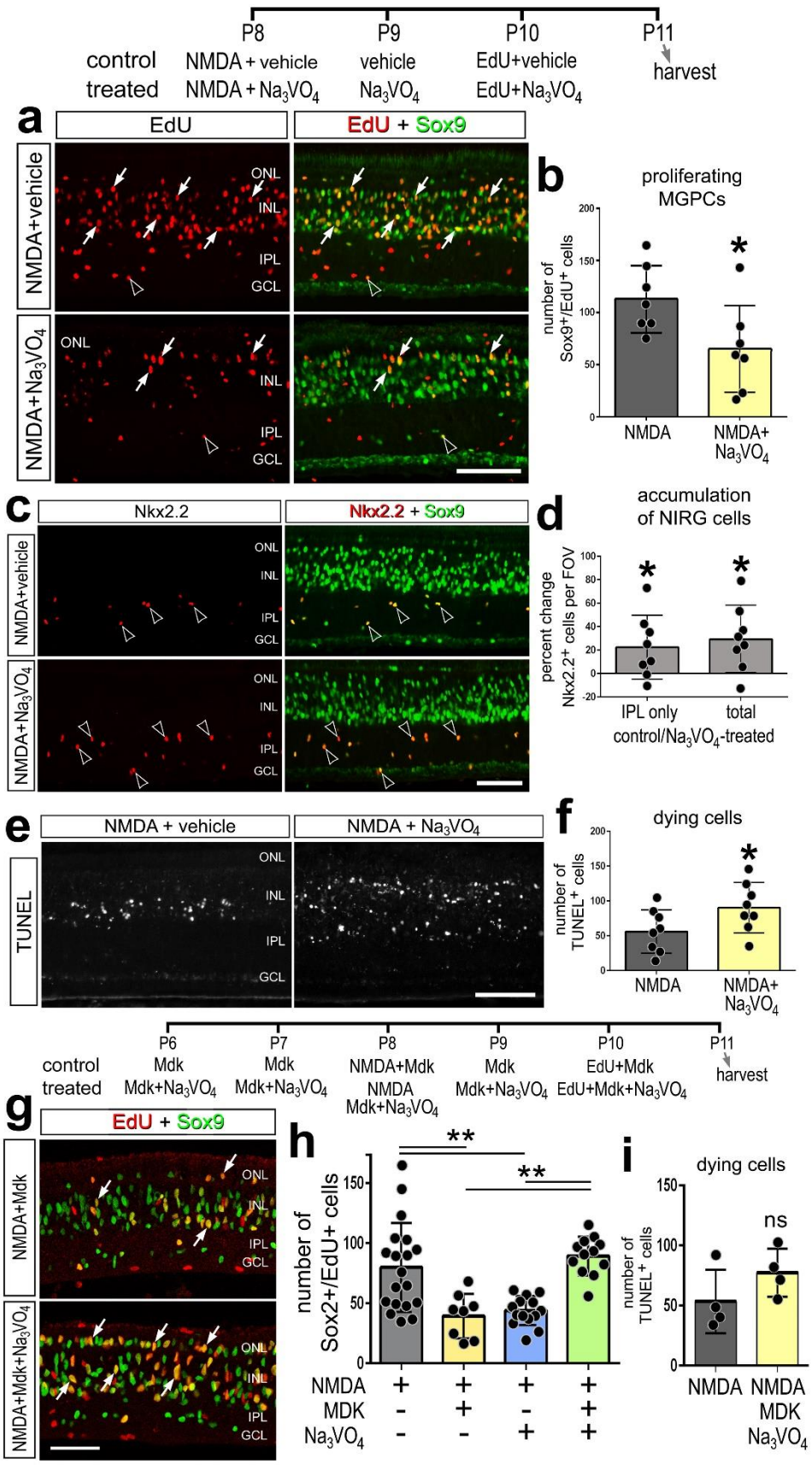
P8
P9
P10
P11
control
treated
NMDA + vehicle
NMDA + Na3VO4
vehicle
Na3VO4
EdU+vehicle
EdU+Na3VO4
harvest
a
EdU
EdU + Sox9
NMDA+vehicle
NMDA+Na3VO4
ONL
INL
IPL
GCL
b
proliferating MGPCs
number of Sox9+/EdU+ cells
NMDA
NMDA+ Na3VO4
c
Nkx2.2
Nkx2.2 + Sox9
d
accumulation of NIRG cells
percent change Nkx2.2+ cells per FOV
IPL only
total
control/Na3VO4-treated
e
NMDA + vehicle
NMDA + Na3VO4
TUNEL
f
dying cells
number of TUNEL+ cells
P6
P7
P8
P9
P10
P11
Mdk
Mdk+Na3VO4
NMDA+Mdk
NMDA Mdk+Na3VO4
EdU+Mdk
EdU+Mdk+Na3VO4
g
NMDA+Mdk
NMDA+Mdk+Na3VO4
h
number of Sox2+/EdU+ cells
NMDA
MDK
Na3VO4
i
dying cells
ns
number of TUNEL+ cells

1166

Figure 6. Patterns of expression and inhibition of putative MDK receptors, integrins, and signal transducers in damaged retinas. scRNA-seq libraries (Fig. 2) were probed for patterns of expression of integrin alpha/beta isoforms and associated signaling ITGB1 molecules p21 associated kinase-1 (PAK1), protein phosphatase 2a catalytic subunit alpha (PPP2CA), integrin linked kinase (ILK), and ARF GTPase-activating protein (GIT1). tSNE plots demonstrate patterns of expression of *PAK1, ITGB1, ITGA1, ITGA2, ITGA3, ITGA6, ITGAV, CAT, CDC42, GIT1, ILK* and *PPP2CA* (**a**). Violin/scatter plots indicate significant differences (*p<0.01, **p<0.001, ***p<<0.001; Wilcox rank sum with Bonferoni correction) in expression of *PAK1, ITGB1, ITGA1, ITGA2, ITGA3, ITGA6, ITGAV, CAT, CDC42, GIT1, ILK* and *PPP2CA* among MG and MGPCs (**b**). The number on each violin indicates the percentage of expressing cells. PAK1-specific inhibitor IPA3 was injected with and following NMDA (**c**,**d**) or before NMDA (**e**) and analyzed for proliferation of MGPCs. Alternatively, PP2A-specific inhibitors calyculin A or fostriecin were injected with and following NMDA (**f**-**h**). Sections of the retina were labeled for EdU (red) and Sox9 (green; **c, f**). Arrows indicate nuclei of proliferating MGPCs (**a,g**). The histogram/scatter-plots in **d, e, g** and **h** illustrate the mean (±SD) number of labeled cells. Each dot represents one biological replicate. Significance of difference (*p<0.05) was determined by using a paired *t*-test. Arrows indicate nuclei of proliferating MGPCs (**c,f**). The calibration bar panels **c** and **f** represent 50 µm. Abbreviations: ONL – outer nuclear layer, INL – inner nuclear layer, IPL – inner plexiform layer, GCL – ganglion cell layer, ns – not significant.

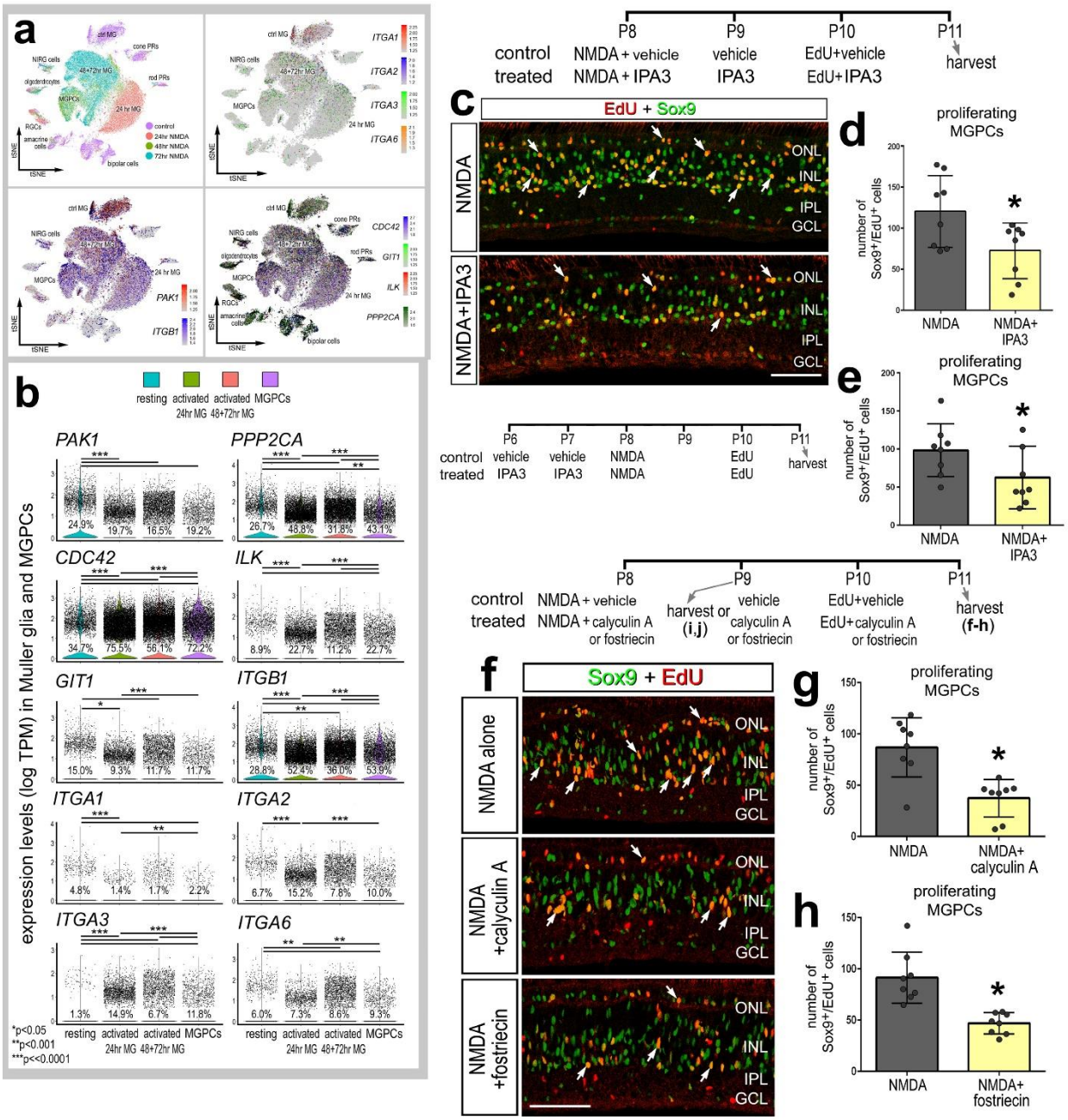
a
ctrl MG
cone PRs
NIRG cells
48+72hr MG
rod PRs
oligodendrocytes
MGPCs
24 hr MG
RGCs
amacrine cells
bipolar cells
control
24hr NMDA
48hr NMDA
72hr NMDA
tSNE
ITGA1
ITGA2
ITGA3
ITGA6
PAK1
ITGB1
CDC42
GIT1
ILK
PPP2CA
b
resting
activated 24hr MG
activated 48+72hr MG
MGPCs
expression levels (log TPM) in Muller glia and MGPCs
PAK1
PPP2CA
CDC42
ILK
GIT1
ITGB1
ITGA1
ITGA2
ITGA3
ITGA6
*p<0.05
**p<0.001
***p<<0.0001
P8
P9
P10
P11
control
treated
NMDA + vehicle
NMDA + IPA3
vehicle
IPA3
EdU+vehicle
EdU+IPA3
harvest
c
EdU + Sox9
NMDA
NMDA+IPA3
ONL
INL
IPL
GCL
d
proliferating MGPCs
number of Sox9+/EdU+ cells
NMDA
NMDA+ IPA3
P6
P7
P8
P9
P10
P11
vehicle IPA3
NMDA NMDA
EdU EdU
e
NMDA + calyculin A or fostriecin
harvest or (i,j)
vehicle calyculin A or fostriecin
EdU+calyculin A or fostriecin
harvest (f-h)
f
Sox9 + EdU
NMDA alone
NMDA +calyculin A
NMDA +fostriecin
g
NMDA+ calyculin A
h
NMDA+ fostriecin

Figure 7. MG expression of *MDK* and putative MDK-receptors in retinas treated with insulin and FGF2. scRNA-seq was used to identify patterns of expression of MDK-related genes among cells in saline-treated retinas and in retinas after 2 and 3 consecutive doses of FGF2 and insulin (**a,b**). In UMAP plots, each dot represents one cell, and expressing cells indicated by colored heatmaps of gene expression for *MDK, PTN, PAK1, CSPG5* and *ITGB1* (**c,d**). Black dots indicate cells with expression of two or more genes. (**e**) Changes in gene expression among UMAP clusters of MG and MGPCs are illustrated with violin plots and significance of difference (*$p<0.1$, **$p<0.0001$, ***$p<<0.0001$) determined using a Wilcox rank sum with Bonferoni correction. The number on each violin indicates the percentage of expressing cells.

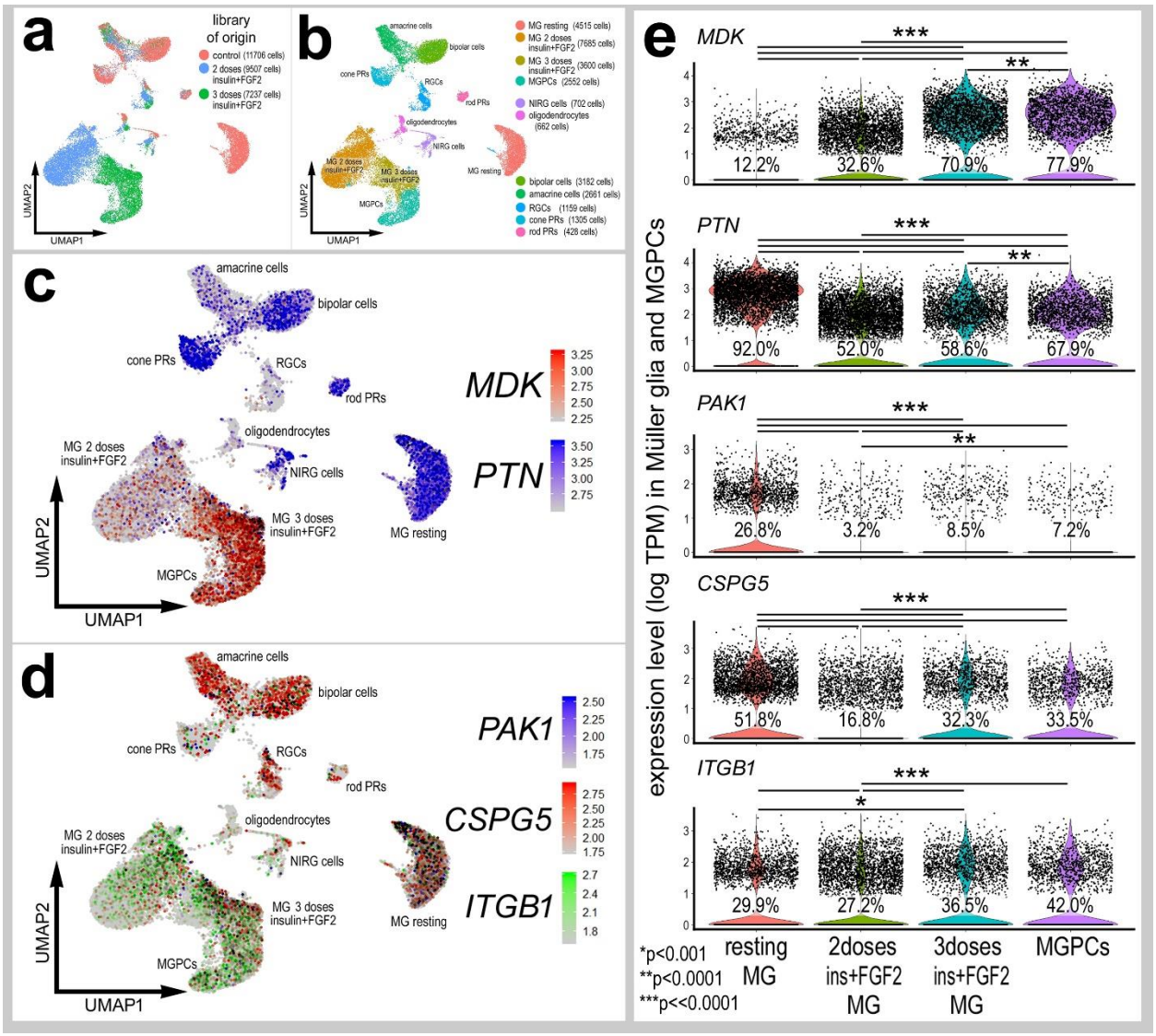
a
library of origin
control (11706 cells)
2 doses (9507 cells) insulin+FGF2
3 doses (7237 cells) insulin+FGF2
UMAP2
UMAP1
b
amacrine cells
bipolar cells
cone PRs
RGCs
rod PRs
oligodendrocytes
NIRG cells
MG 2 doses insulin+FGF2
MG 3 doses insulin+FGF2
MG resting
MGPCs
MG resting (4515 cells)
MG 2 doses insulin+FGF2 (7685 cells)
MG 3 doses insulin+FGF2 (3600 cells)
MGPCs (2552 cells)
NIRG cells (702 cells)
oligodendrocytes (662 cells)
bipolar cells (3182 cells)
amacrine cells (2661 cells)
RGCs (1159 cells)
cone PRs (1305 cells)
rod PRs (428 cells)
c
MDK
3.25
3.00
2.75
2.50
2.25
PTN
3.50
3.25
3.00
2.75
d
PAK1
2.50
2.25
2.00
1.75
CSPG5
2.75
2.50
2.25
2.00
1.75
ITGB1
2.7
2.4
2.1
1.8
e
MDK
PTN
PAK1
CSPG5
ITGB1
expression level (log TPM) in Müller glia and MGPCs
12.2%
32.6%
70.9%
77.9%
92.0%
52.0%
58.6%
67.9%
26.8%
3.2%
8.5%
7.2%
51.8%
16.8%
32.3%
33.5%
29.9%
27.2%
36.5%
42.0%
*p<0.001
**p<0.0001
***p<<0.0001
resting MG
2doses ins+FGF2 MG
3doses ins+FGF2 MG
MGPCs

Figure 8. Expression of *MDK* and MDK-related genes in aggregate of scRNA-seq libraries for MG from different treatments. In UMAP and violin plots each dot represents one cell. MG were bioinformatically isolated from 2 biological replicates for control retinas and retinas treated with 2 doses of insulin and FGF2, 3 doses of insulin and FGF2, 24 hrs after NMDA, 48 hrs after NMDA, 48hrs after NMDA + insulin and FGF2, and 72 hrs after NMDA. UMAP analysis revealed distinct clusters of MG which includes control/resting MG, activated MG from retinas 24hrs after NMDA treatment, activated MG from 2 doses of insulin and FGF2, activated MG from 3 doses of insulin FGF2 and NMDA at different times after treatment, activated MG returning toward a resting phenotype from 48 and 72 hrs after NMDA-treatment, and 3 regions of MGPCs. The dot plot in **c** illustrates some of the pattern-distinguishing genes and relative levels across the different UMAP-clustered MG and MGPCs. UMAP plots illustrate the distinct and elevated expression of *GLUL, RLBP, VIM* and *SLC1A3* in resting MG (**d**) and *CDK1, TOP2A, PCNA* and *SPC25* in different regions of MGPCs (**e**). Violin plots in **f** illustrate relative expression levels for *MDK, PTN, SDC4, PAK1, CSPG5, ITGB1, PPP2CA* and *CDC4* in UMAP-clustered MG and MGPCs. Significance of difference (**$p<0.001$, ***$p<<0.001$) was determined by using a Wilcox rank sum with Bonferoni correction. The number on each violin indicates the percentage of expressing cells.

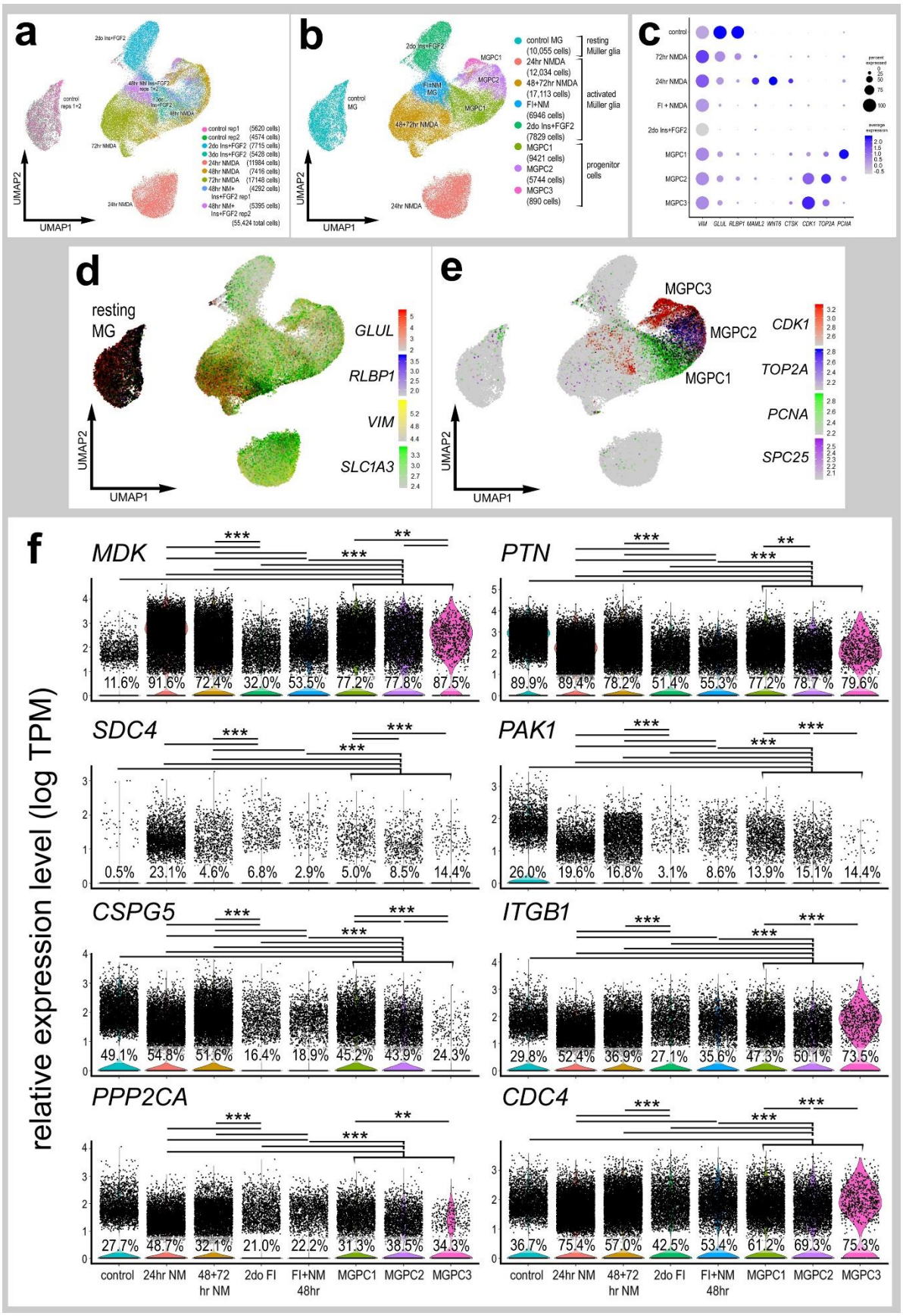
a
b
c
d
e
f
UMAP1
UMAP2
control MG (10,055 cells)
24hr NMDA (12,034 cells)
48+72hr NMDA (17,113 cells)
FI+NM (6946 cells)
2do Ins+FGF2 (7829 cells)
MGPC1 (9421 cells)
MGPC2 (5744 cells)
MGPC3 (890 cells)
resting Müller glia
activated Müller glia
progenitor cells
VIM GLUL RLBP1 MAML2 WNT6 CTSK CDK1 TOP2A PCNA
resting MG
GLUL
RLBP1
VIM
SLC1A3
CDK1
TOP2A
PCNA
SPC25
relative expression level (log TPM)
MDK
PTN
SDC4
PAK1
CSPG5
ITGB1
PPP2CA
CDC4
control
24hr NM
48+72 hr NM
2do FI
FI+NM 48hr
MGPC1
MGPC2
MGPC3

Figure 9. The combination of MDK with FGF2 and insulin had no effect on the formation of proliferating MGPCs. (**a**-**h**) Retinas were obtained from eyes that received 2 consecutive daily doses of vehicle or MDK/IPA3, 3 consecutive daily injections of FGF2 and insulin with or without MDK/IPA3, followed by an injection of EdU, and harvested 24 hrs after the final injection. (**i**-**j**) Alternatively, retinas were obtained from eyes that received, 3 consecutive daily injections of FGF2 and insulin with or without $NaVO_4$, followed by 2 consecutive daily injections of EdU, and harvested 24 hrs after the final injection. The responses of MG, microglia, and NIRG proliferation and accumulation was evaluated after harvesting. Sections of the retina were labeled for EdU (red; **a**), TUNEL(**l**) or antibodies to Sox9 (green; **a**, **j**) and Nkx2.2 (red; **j**). The histogram/scatter-plots illustrate the mean (±SD) number of proliferating MGPCs, microglia, NIRG cells, or TUNEL positive nuclei. Significance of difference (*$p<0.05$) was determined by using a *t*-test. Arrows indicate $EdU^+/Sox9^+$ MG, small double-arrows indicate proliferating NIRG cells, and hollow arrow-heads indicate $Sox9^+/Nkx2.2^+$ NIRG cells. The calibration bars in panels **a** and **j** represent 50 µm. Abbreviations: ONL – outer nuclear layer, INL – inner nuclear layer, IPL – inner plexiform layer, GCL – ganglion cell layer.

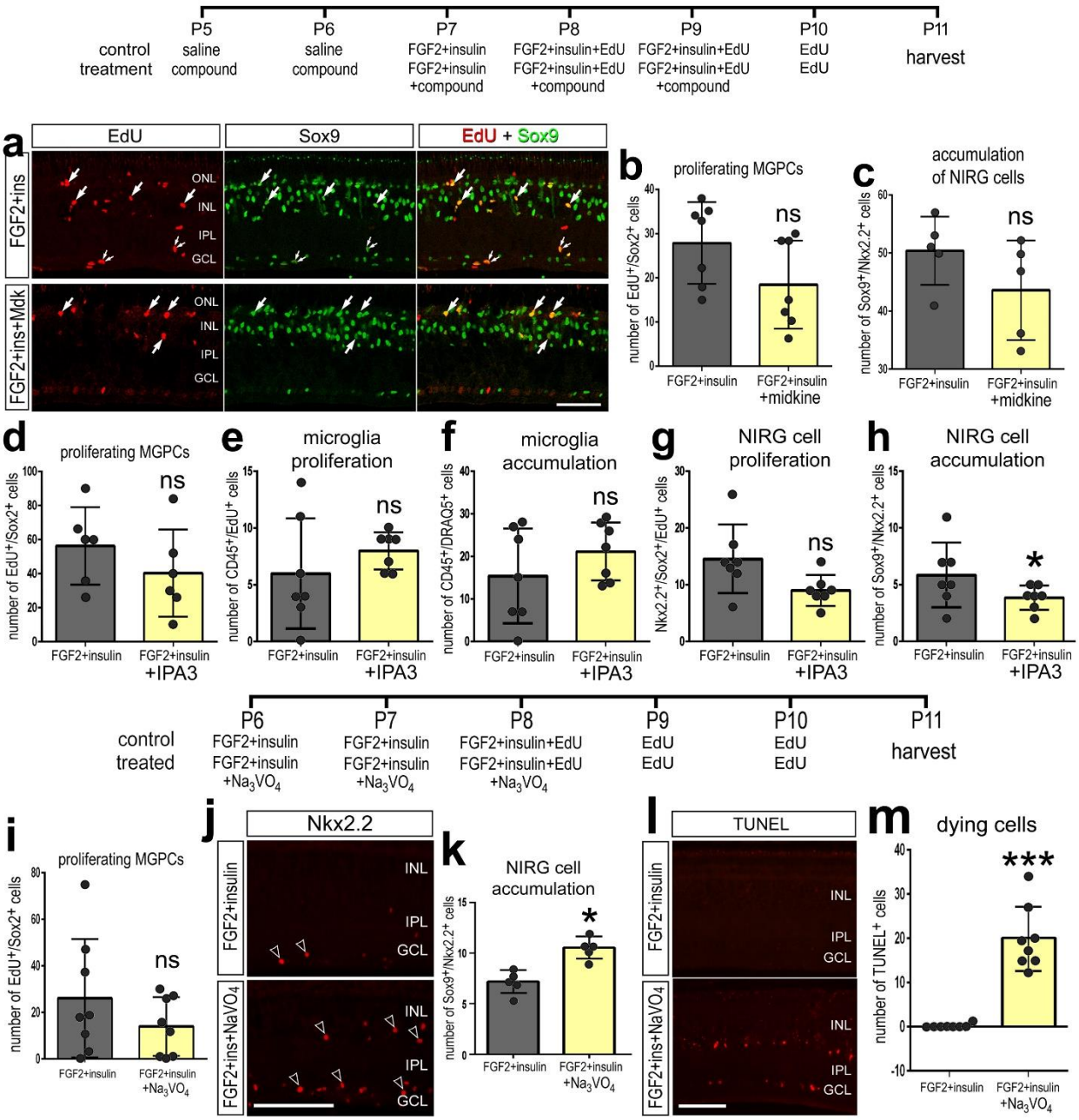
P5
P6
P7
P8
P9
P10
P11
control treatment
saline compound
saline compound
FGF2+insulin FGF2+insulin +compound
FGF2+insulin+EdU FGF2+insulin+EdU +compound
FGF2+insulin+EdU FGF2+insulin+EdU +compound
EdU EdU
harvest
a
EdU
Sox9
EdU + Sox9
FGF2+ins
FGF2+ins+Mdk
ONL
INL
IPL
GCL
b
proliferating MGPCs
number of EdU+/Sox2+ cells
ns
FGF2+insulin
FGF2+insulin +midkine
c
accumulation of NIRG cells
number of Sox9+/Nkx2.2+ cells
ns
FGF2+insulin
FGF2+insulin +midkine
d
proliferating MGPCs
number of EdU+/Sox2+ cells
ns
FGF2+insulin
FGF2+insulin +IPA3
e
microglia proliferation
number of CD45+/EdU+ cells
ns
FGF2+insulin
FGF2+insulin +IPA3
f
microglia accumulation
number of CD45+/DRAQ5+ cells
ns
FGF2+insulin
FGF2+insulin +IPA3
g
NIRG cell proliferation
Nkx2.2+/Sox2+/EdU+ cells
ns
FGF2+insulin
FGF2+insulin +IPA3
h
NIRG cell accumulation
number of Sox9+/Nkx2.2+ cells
*
FGF2+insulin
FGF2+insulin +IPA3
control treated
P6
P7
P8
P9
P10
P11
FGF2+insulin FGF2+insulin +Na3VO4
FGF2+insulin FGF2+insulin +Na3VO4
FGF2+insulin+EdU FGF2+insulin+EdU +Na3VO4
EdU EdU
EdU EdU
harvest
i
proliferating MGPCs
number of EdU+/Sox2+ cells
ns
FGF2+insulin
FGF2+insulin +Na3VO4
j
Nkx2.2
FGF2+insulin
FGF2+ins+NaVO4
INL
IPL
GCL
k
NIRG cell accumulation
number of Sox9+/Nkx2.2+ cells
*
FGF2+insulin
FGF2+insulin +Na3VO4
l
TUNEL
FGF2+insulin
FGF2+ins+NaVO4
INL
IPL
GCL
m
dying cells
number of TUNEL+ cells
***
FGF2+insulin
FGF2+insulin +Na3VO4

Figure 10. Mouse MG have a reduced profile of *Mdk*, *Ptn* and MDK-related genes in MG in response to NMDA damage. Cells were obtained from control retinas and from retinas at 3, 6, 12, 24, 36, 48 and 72hrs after NMDA-treatment and clustered in UMAP plots with each dot representing an individual cell (**a**). UMAP plots revealed distinct clustering of different types of retinal cells; resting MG (a mix of control, 48hr and 72hr NMDA-tr), 12-72 hr NMDA-tr MG (activated MG in violin plots), 6hrs NMDA-tr MG, 3hrs NMDA-tr MG, microglia, astrocytes, RPE cells, endothelial cells, retinal ganglion cells, horizontal cells (HCs), amacrine cells (ACs), bipolar cells (BPs), rod photoreceptors, and cone photoreceptors (**b**). Cells were colored with a heatmap of expression of *Mdk, Ptn, Sdc4, Pak1, Ptprz1, Cspg5, Itgb1bp1, Itga4* and *Itgba6* gene expression (**c**). Black dots indicates cells with two or more markers. In MG, changes in gene expression are illustrated with violin/scatter plots of *Mdk, Ptn, Pak1, Cspg5, Sdc4, and Itgb1* and quantified for significant changes (**d**) (*p<0.01, **p<0.0001, ***p<<0.001). Similarly, UMAP-clustered microglia were analyzed and genes *Itgb1* and *Itga6* were detected and quantified in violin plots for cells from each library of origin (**e**). The number on each violin indicates the percentage of expressing cells.

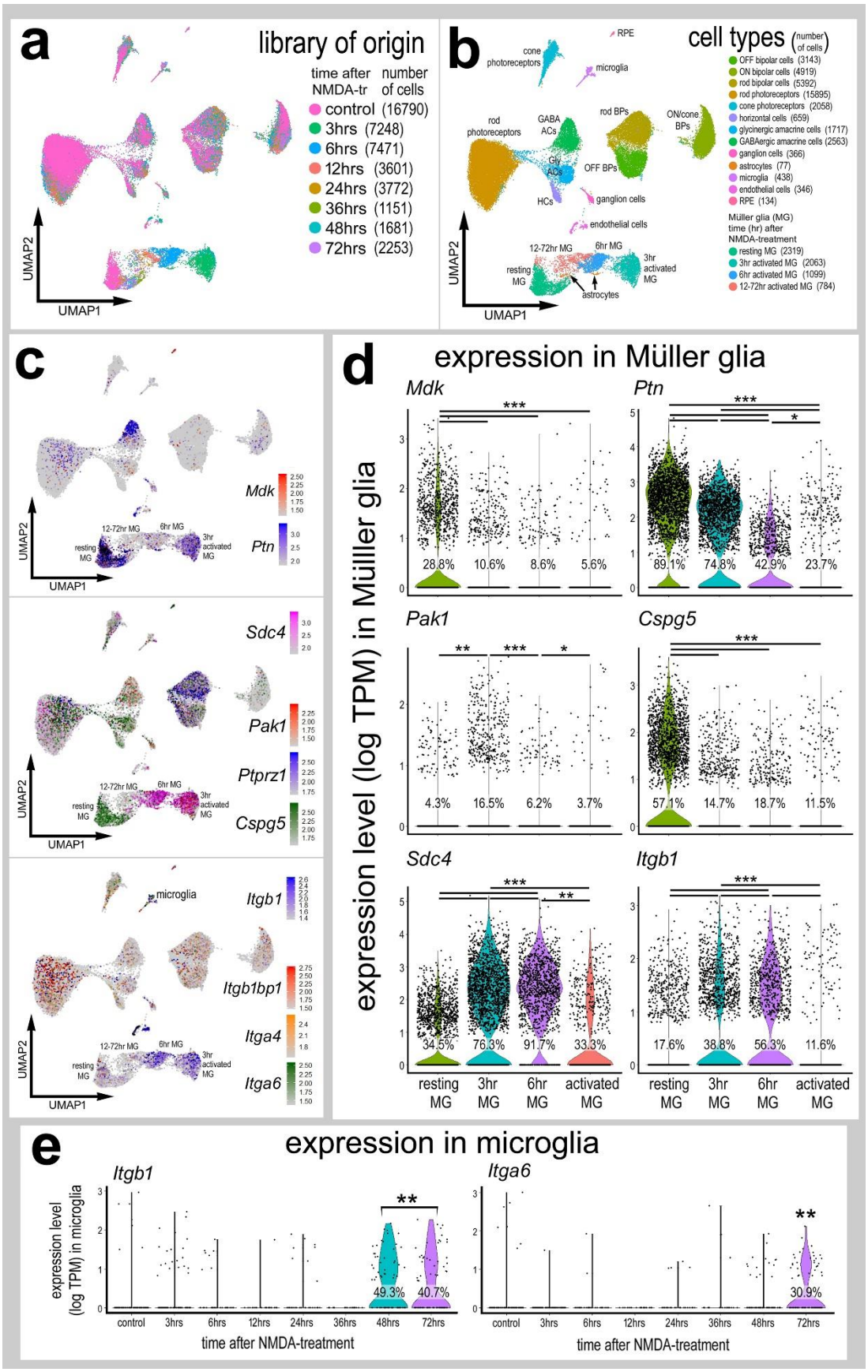
a
library of origin
time after NMDA-tr
number of cells
control (16790)
3hrs (7248)
6hrs (7471)
12hrs (3601)
24hrs (3772)
36hrs (1151)
48hrs (1681)
72hrs (2253)
UMAP2
UMAP1
b
cell types (number of cells)
RPE
cone photoreceptors
microglia
rod photoreceptors
GABA ACs
rod BPs
ON/cone BPs
Gly ACs
OFF BPs
HCs
ganglion cells
endothelial cells
12-72hr MG
6hr MG
resting MG
3hr activated MG
astrocytes
OFF bipolar cells (3143)
ON bipolar cells (4919)
rod bipolar cells (5392)
rod photoreceptors (15895)
cone photoreceptors (2058)
horizontal cells (659)
glycinergic amacrine cells (1717)
GABAergic amacrine cells (2563)
ganglion cells (366)
astrocytes (77)
microglia (438)
endothelial cells (346)
RPE (134)
Müller glia (MG) time (hr) after NMDA-treatment
resting MG (2319)
3hr activated MG (2063)
6hr activated MG (1099)
12-72hr activated MG (784)
c
Mdk
Ptn
Sdc4
Pak1
Ptprz1
Cspg5
Itgb1
Itgb1bp1
Itga4
Itga6
d
expression in Müller glia
expression level (log TPM) in Müller glia
Mdk
Ptn
Pak1
Cspg5
Sdc4
Itgb1
28.8%
10.6%
8.6%
5.6%
89.1%
74.8%
42.9%
23.7%
4.3%
16.5%
6.2%
3.7%
57.1%
14.7%
18.7%
11.5%
34.5%
76.3%
91.7%
33.3%
17.6%
38.8%
56.3%
11.6%
resting MG
3hr MG
6hr MG
activated MG
e
expression in microglia
Itgb1
Itga6
expression level (log TPM) in microglia
49.3%
40.7%
30.9%
control
3hrs
6hrs
12hrs
24hrs
36hrs
48hrs
72hrs
time after NMDA-treatment

1260

Figure 11. MDK activates cell-signaling in MG and stimulates proliferation in the mouse retina. (**a**-**e**) A single intraocular injection of MDK was delivered and retinas were harvested 4 hours later. The histogram in **a** represents the mean percent change (±SD) in density sum and area for percentage change in intensity sum for cFOS and pS6 immunofluorescence. Each dot represents one replicate retina. Significance of difference (**$p<0.01$, ***$p<0.0001$) was determined by using a paired two-way *t*-test. Vertical sections of saline (control) and MDK-treated retinas were labeled with antibodies to cFOS (green; **b**,**c**), pS6 (green; **d**,**e**) and Sox2 (magenta; **c**,**e**). (**f**-**h**) Treatment included intraocular injections of MDK or vehicle at P60, NMDA and MDK/vehicle at P62, MDK or vehicle at P60, Edu was applied daily by intraperitoneal (IP) injections from P62 through P66, and tissues were harvested at P67. The histogram in **h** represents the mean (±SD) numbers of $EdU^+/Sox9^+$ cells in the INL. Each dot represents one replicate retina. Significance of difference (*$p<0.05$) was determined by using a paired two-way *t*-test. Arrows indicate the nuclei of MG and arrow-heads indicate $EdU^+/Sox9^-$ cells (presumptive proliferating microglia). The calibration bar (50 µm) in panel **d** applies to **b** and **d**. Abbreviations: ONL – outer nuclear layer, INL – inner nuclear layer, IPL – inner plexiform layer, GCL – ganglion cell layer.

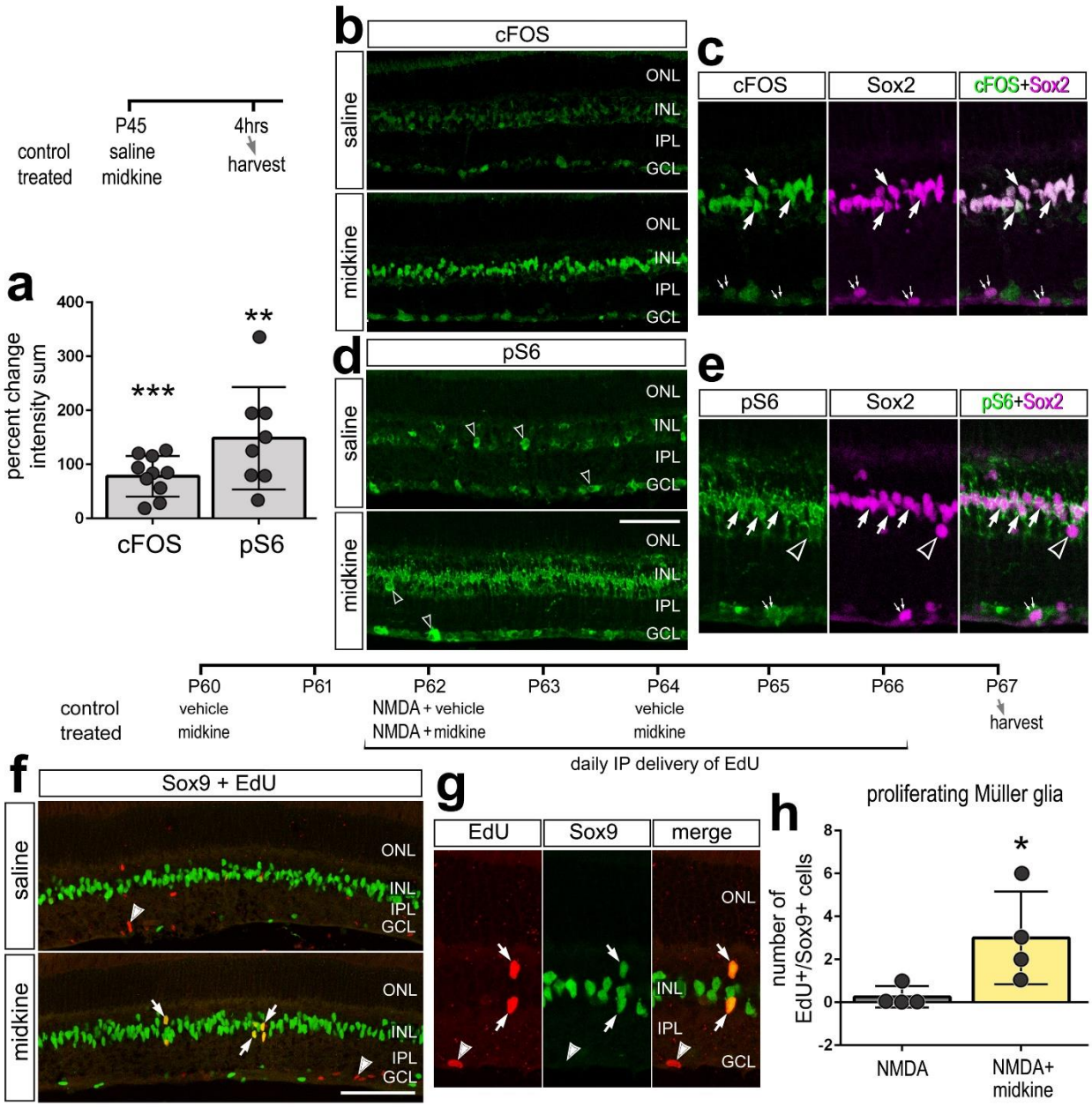
control
treated
P45
saline
midkine
4hrs
harvest
a
percent change intensity sum
400
300
200
100
0
***
**
cFOS
pS6
b
cFOS
saline
midkine
ONL
INL
IPL
GCL
c
cFOS
Sox2
cFOS+Sox2
d
pS6
e
pS6
Sox2
pS6+Sox2
P60
P61
P62
P63
P64
P65
P66
P67
vehicle
midkine
NMDA + vehicle
NMDA + midkine
daily IP delivery of EdU
f
Sox9 + EdU
g
EdU
Sox9
merge
h
proliferating Müller glia
number of EdU+/Sox9+ cells
8
6
4
2
0
-2
NMDA
NMDA+ midkine

Figure 12. Schematic summary of MDK-signaling in normal and NMDA-damaged retinas. Patterns of expression, determined by scRNA-seq, are shown for Integrin β1, Integrin α, PTPRZ1, PAK1 and MDK in MG, NIRG cells and inner retinal neurons. Although GIT1, ILK, CDC42, and PP2A (*PPP2CA)* were widely expressed by nearly all retinal cells (according to scRNA-seq data; see Fig 6a), signaling through Integrins is shown only in MG because *ITG's* were largely confined to MG. Putative sites of action are shown for small-molecule inhibitors, including IPA3, calyculin A, fostriecin and Na_3VO_4. Abbreviations: PRL – photoreceptor layer, ONL – outer nuclear layer, INL – inner nuclear layer, IPL – inner plexiform layer, GCL – ganglion cell layer, NFL – nerve fiber layer.

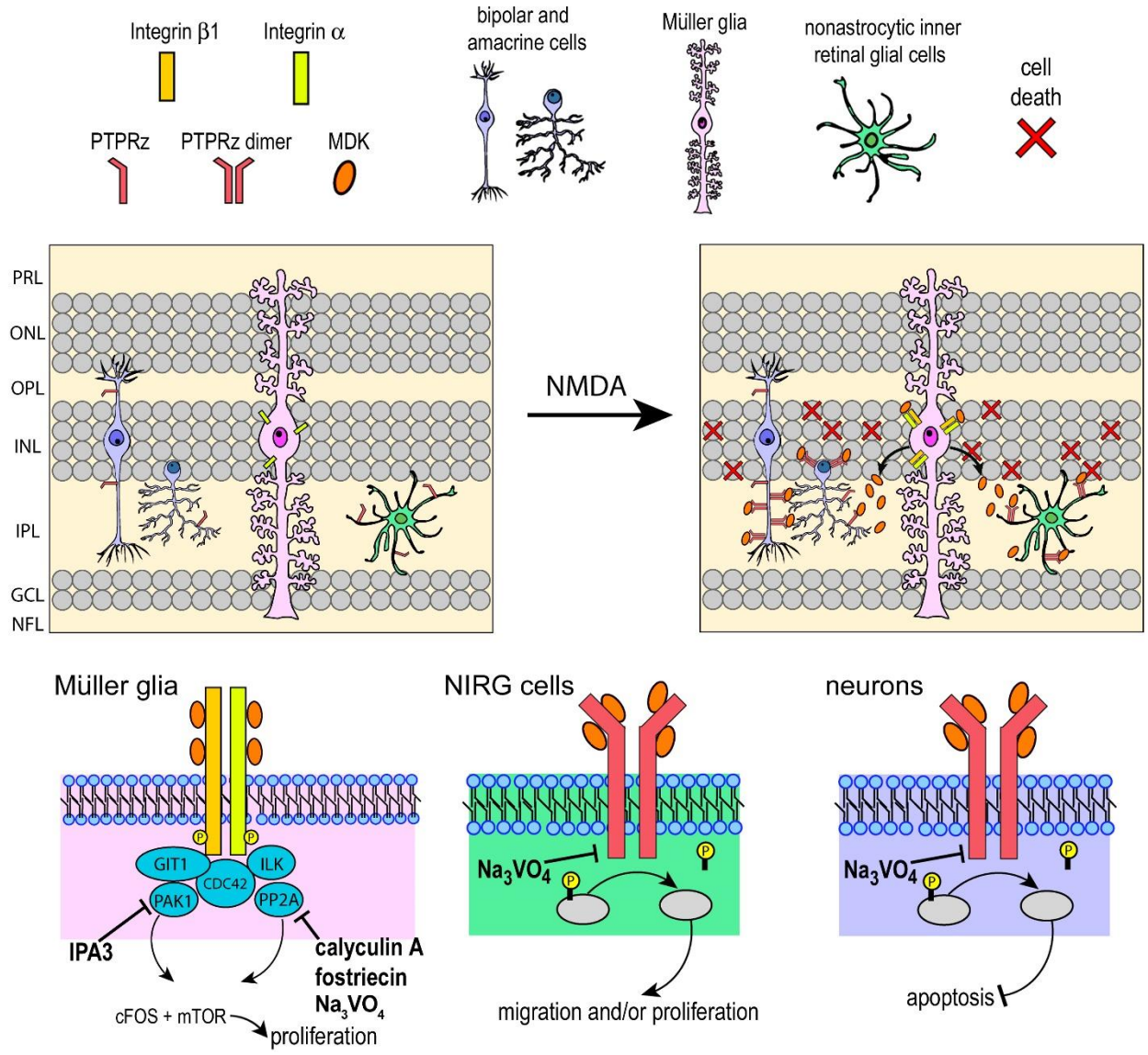
Integrin β1
Integrin α
PTPRz
PTPRz dimer
MDK
bipolar and amacrine cells
Müller glia
nonastrocytic inner retinal glial cells
cell death
PRL
ONL
OPL
INL
IPL
GCL
NFL
NMDA
Müller glia
GIT1
ILK
CDC42
PAK1
PP2A
IPA3
calyculin A
fostriecin
Na3VO4
cFOS + mTOR
proliferation
NIRG cells
Na3VO4
migration and/or proliferation
neurons
Na3VO4
apoptosis